

1 **Conversion of coastal wetland to aquaculture ponds decreased**  
2 **N<sub>2</sub>O emission: Evidence from a multi-year field study**

3 Ping Yang<sup>a,b\*</sup>, Kam W. Tang<sup>c</sup>, Chuan Tong<sup>a,b\*</sup>, Derrick Y.F. Lai<sup>d</sup>, Linhai  
4 Zhang<sup>a,b</sup>, Xiao Lin<sup>a,b</sup>, Hong Yang<sup>e,f</sup>, Lishan Tan<sup>g</sup>, Yifei Zhang<sup>a</sup>, Yan Hong<sup>a</sup>,  
5 Chen Tang<sup>a</sup>, Yongxin Lin<sup>a,b\*</sup>

6 <sup>a</sup>*School of Geographical Sciences, Fujian Normal University, Fuzhou 350007,*  
7 *P.R. China*

8 <sup>b</sup>*Key Laboratory of Humid Subtropical Eco-geographical Process of Ministry of*  
9 *Education, Fujian Normal University, Fuzhou 350007, P.R. China*

10 <sup>c</sup>*Department of Biosciences, Swansea University, Swansea SA2 8PP, U. K.*

11 <sup>d</sup>*Department of Geography and Resource Management, The Chinese University of*  
12 *Hong Kong, Hong Kong, China*

13 <sup>e</sup>*College of Environmental Science and Engineering, Fujian Normal University, Fuzhou*  
14 *350007, P.R. China*

15 <sup>f</sup>*Department of Geography and Environmental Science, University of Reading, Reading,*  
16 *RG6 6AB, UK*

17 <sup>h</sup>*State Key Laboratory of Estuarine and Coastal Research, East China Normal*  
18 *University, Shanghai, China*

19

20 **\*Correspondence to:**

21 Ping Yang ([yangping528@sina.cn](mailto:yangping528@sina.cn)); Chuan Tong ([tongch@fjnu.edu.cn](mailto:tongch@fjnu.edu.cn)); Yongxin Lin  
22 ([yxlin@fjnu.edu.cn](mailto:yxlin@fjnu.edu.cn))

23 **Telephone:** 086-0591-87445659 **Fax:** 086-0591-83465397

## 24 ABSTRACT

25 Land reclamation is a major threat to the world's coastal wetlands, and it may influence  
26 the biogeochemical cycling of nitrogen in coastal regions. Conversion of coastal  
27 marshes into aquaculture ponds is common in the Asian Pacific region, but its impacts  
28 on the production and emission of nitrogen greenhouse gases remain poorly understood.  
29 In this study, we compared N<sub>2</sub>O emission from a brackish marsh and converted shrimp  
30 aquaculture ponds in the Shanyutan wetland, the Min River Estuary in Southeast China  
31 over a three-year period. We also measured sediment and porewater properties, relevant  
32 functional gene abundance, sediment N<sub>2</sub>O production potential and denitrification  
33 potential in the two habitats. Results indicated that the pond sediment had lower  
34 N-substrate availability, lower ammonia oxidation (AOA and comammox *Nitrospira*  
35 *amoA*), nitrite reduction (*nirK* and *nirS*) and nitrous oxide reduction (*nosZ* I and *nosZ* II)  
36 gene abundance and lower N<sub>2</sub>O production and denitrification potentials than in marsh  
37 sediments. Consequently, N<sub>2</sub>O emission fluxes from the aquaculture ponds (range 5.4–  
38 251.8 μg m<sup>-2</sup> h<sup>-1</sup>) were significantly lower than those from the marsh (12.6–570.7 μg m<sup>-2</sup>  
39 h<sup>-1</sup>). Overall, our results show that conversion from marsh to shrimp aquaculture ponds  
40 in the Shanyutan wetland may have diminished nutrient input from the catchment,  
41 impacted the N-cycling microbial community and lowered N<sub>2</sub>O production capacity of  
42 the sediment, leading to lower N<sub>2</sub>O emissions. Better post-harvesting management of  
43 pond water and sediment may further mitigate N<sub>2</sub>O emissions caused by the aquaculture  
44 operation.

45 **Keywords:** Nitrogen substrate; Nitrification and denitrification; Nitrous oxide (N<sub>2</sub>O)  
46 production; N<sub>2</sub>O fluxes; Coastal wetlands; Aquaculture reclamation

## 47 **1. Introduction**

48 Nitrous oxide (N<sub>2</sub>O) is a kind of the potent long-lived greenhouse gases with 270  
49 times the global warming potential of carbon dioxide (CO<sub>2</sub>) on a 100-year timescale  
50 (Neubauer and Megonigal, 2015), and it causes major destruction of stratospheric  
51 ozone (Ravishankara et al., 2009; Shaaban et al., 2018). The recent report by the World  
52 Meteorological Organization (WMO) showed that the global atmospheric N<sub>2</sub>O  
53 concentration has been increasing since 1750, reaching 333 ppbv in 2020 (WMO,  
54 2019). Land use and land cover change (LULCC) is considered an important driver of  
55 anthropogenic N<sub>2</sub>O emission (Gutlein et al., 2018; IPCC, 2013); thus, good  
56 understanding of the effects of LULCC on N<sub>2</sub>O emission from various ecosystems is  
57 essential for mitigating climate change (Tan et al., 2020; Webb et al., 2021; Zhou et al.,  
58 2019).

59 Coastal wetlands, located at the interface of land and sea, typically have high  
60 biological productivity (Chmura et al., 2003; He et al., 2021) and are an important  
61 nitrogen pool in the global nitrogen cycle (Batjes, 1996; Wu et al., 2013). Over the past  
62 century, land conversion to accommodate population growth and economic  
63 development has led to the loss or degradation of large areas of natural wetlands  
64 globally (Sun et al., 2015; Verhoeven and Setter, 2010). Conversion of wetlands to  
65 aquaculture ponds for food production is common around the world (He et al., 2021;  
66 Gao et al., 2019; Murray et al., 2019), particularly in the Asia-Pacific region. China is  
67 one of the major aquaculture producers in the world (FAO, 2020). Aquaculture ponds

68 are estimated to cover a total area of 15,600 km<sup>2</sup> in China (Duan et al., 2020), most of  
69 which were reclaimed from coastal wetlands by removing the original vegetation and  
70 converting the bunds into steep slopes (Yang et al., 2017). This alteration of the  
71 landscape, from vegetated areas with shallow free-flowing water to isolated standing  
72 water bodies, can strongly affect nutrient cycles, sediment properties, abundance and  
73 activity of N-cycling microorganisms and subsequent N<sub>2</sub>O biogeochemical processes  
74 (Huang et al., 2010; Jiang et al., 2009; Roulet, 2000), but long-term data on the  
75 direction and magnitude of these effects are lacking.

76 To investigate the climate effect of LULCC, ideally one should monitor N<sub>2</sub>O  
77 production and emissions from the location before and after the creation of aquaculture  
78 ponds. However, this is impossible for existing ponds. As an alternative, one may  
79 compare N<sub>2</sub>O production and emission from the aquaculture ponds and the surrounding  
80 native habitat. To that end, we compared N<sub>2</sub>O emission fluxes between a brackish  
81 marsh and converted aquaculture ponds in the Shanyutan wetland, Southeast China  
82 over a three-year period. To explore the underlying factors that may explain the  
83 differences, we measured sediment and porewater properties, major N-cycling  
84 functional genes, sediment N<sub>2</sub>O production and denitrification potentials between the  
85 two habitat types across the shrimp farming season. The main research objectives are to:  
86 (1) investigate differences in the sediment N<sub>2</sub>O production and denitrification potentials  
87 and the relevant bacterial gene abundance between marsh land and aquaculture ponds;  
88 (2) assess the effects of marsh land conversion on N<sub>2</sub>O emissions; (3) identify the main

89 environmental factors influencing the change in N<sub>2</sub>O emissions. We hypothesized that  
90 the conversion of coastal marsh to aquaculture ponds would decrease the N<sub>2</sub>O  
91 emissions by changing the hydrological and edaphic conditions.

## 92 **2. Materials and methods**

### 93 *2.1. Study area*

94 The Shanyutan wetland (26°00'36" to 26°03'42"N, 119°34'12" to 119°40'40"E) is  
95 located in the Min River Estuary (MRE), Southeast China (Figure 1). The region has a  
96 typical subtropical monsoonal climate. The annual mean air temperature is 19.6 °C and  
97 annual average precipitation is 1,390 mm (Yang et al., 2022a). The wetland is  
98 characterized by typical semidiurnal tides, and tides change in the range of 2.5–6.0 m.  
99 The average water salinity is around 4.2±0.3‰ (Tong et al., 2018). The main vegetation  
100 includes the native *Cyperus malaccensis* (912 stems m<sup>-2</sup> aboveground density and  
101 3168±486 g m<sup>-2</sup> belowground biomass) and *Phragmites australis* (150 stems m<sup>-2</sup>;  
102 2322±533 g m<sup>-2</sup>) and the invasive *Spartina alterniflora* (257 stems m<sup>-2</sup>; 2085±486 g m<sup>-2</sup>)  
103 (Yang et al., 2018). Large areas of the coastal marshes (mainly dominated by *C.*  
104 *malaccensis* and *S. alterniflora*) have been converted to aquaculture ponds in the past  
105 decades due to rising demand for seafood, primarily shrimp (*Litopenaeus vannamei*)  
106 (Yang et al., 2020).

107 The size of the aquaculture ponds varied in the range of 1.2–3.0 ha and mean water  
108 depth was ~1.5 m. Prior to farming, the shrimp ponds were filled with seawater pumped  
109 from the MRE and freshwater drawn locally. Approximately seven days after filling,

110 the pond water was disinfected by using trichloroisocyanuric acid ( $\sim 25$  kg pond<sup>-1</sup>) and  
111 calcium oxide lime ( $0.5$  t ha<sup>-1</sup>), followed by the addition of calcium superphosphate  
112 fertilizer ( $1.5$ – $2.0$  kg per  $1000$  m<sup>3</sup>) (Yang et al., 2022b). There was no water exchange  
113 over the shrimp culture period from breeding in May to harvesting in November (Yang  
114 et al., 2017, 2021). The stocking density was  $150$ – $250$  post larvae m<sup>-2</sup>. Over the farming  
115 period, the shrimp were fed pellets ( $5000$  kg ha<sup>-1</sup>) (Yuehai™, Guangzhou, Guang dong,  
116 China) daily at 08:00 a.m. and 16:00 p.m. Feeds accounted for over 90% of the total N  
117 input, at a rate of  $23.8$ – $33.2$  g N m<sup>-2</sup> yr<sup>-1</sup> (Yang et al., 2021). Similar management  
118 practices are widely applied in coastal shrimp ponds in other regions in China and  
119 Southeast Asia (Herbeck et al., 2013; Kongkeo, 1997; Pouil et al., 2019; Xie and Yu,  
120 2007).

121 To assess the influence of land conversion on sediment N<sub>2</sub>O production and  
122 emissions from the Shanyutan wetland, a brackish *C. malaccensis* marsh stand and  
123 three nearby converted aquaculture ponds were chosen for comparison. Sediment  
124 sampling and incubation were conducted monthly between April 2019 and January  
125 2020 for a total of 10 times. N<sub>2</sub>O emission fluxes were measured between April 2019  
126 and December 2021 in irregular time intervals, subject to Covid-19 related travel  
127 restriction and personnel availability; N<sub>2</sub>O emissions were measured 36 times over the  
128 three-year period.

## 129 2.2. Collection and analysis of sediment porewater

130 In the marsh stand, we established three quadrants ( $1$  m  $\times$   $1$  m)  $2$  m apart. Sediment

131 porewater was collected by using *in situ* dialysis (Strack and Waddington 2008; Tong et  
132 al., 2018). A series of PVC pipes (with inner diameter of 5 cm) with a bottom screen of  
133 0.2  $\mu\text{m}$  nylon membrane (Biotrans<sup>TM</sup>, ICN, Irvine, California, USA) were installed in  
134 each quadrat, extending 15 cm into the sediment and leaving a 5-cm protrusion at the  
135 surface (Yang et al., 2019). The pipe top was sealed with a cover tightly. The porewater  
136 in the pipe was extracted using a syringe (100-mL) with a three-way stopcock. The  
137 collected porewater was immediately transferred into a 100-mL serum glass bottle and  
138 transported to the Key Laboratory of Humid Subtropical Eco-geographical Process of  
139 Ministry of Education (Fuzhou, China) for measurement.

140 To obtain sediment porewater from the aquaculture ponds, 15-cm long sediment  
141 cores were sampled at three sites in each pond using a steel cylinder sampler (5 cm in  
142 diameter). Sediment porewater was extracted by centrifugation at 4,000 rpm for 10 min  
143 (Hereaus Omnifuge 2000 RS, Hereaus, Hanau, Frankfurt, Germany) (Matos et al., 2016)  
144 and transferred into a 100-mL serum glass bottle.

145 All porewater samples were kept cold and dark before measurement. In the  
146 laboratory, ~50 mL porewater was filtered through a 0.45  $\mu\text{m}$  filter (Biotrans<sup>TM</sup> nylon  
147 membranes). The filtrates were measured for ammonia-nitrogen ( $\text{NH}_4^+\text{-N}$ ),  
148 nitrate-nitrogen ( $\text{NO}_3^-\text{-N}$ ), and total dissolved nitrogen (TDN) concentrations using a  
149 flow injection analyzer (Skalar Analytical SAN<sup>++</sup>, Netherlands). Porewater  $\text{SO}_4^{2-}$   
150 concentration was determined by using a Dionex 2100 Ion Chromatograph (Thermo  
151 Fisher Scientific, Sunnyvale, California, USA).

152 2.3. *Collection and analysis of sediment samples*

153 Triplicate 15-cm long sediment cores were collected from the marsh stand and  
154 aquaculture ponds with a steel cylinder sampler (5 cm in diameter). All sediment cores  
155 were put into sterile sample bags, stored on ice in a cooler, and transported back to the  
156 laboratory for further analysis within 4–6 hr. In the laboratory, sediment was diluted  
157 with deionized water for measuring sediment pH (sediment-to-water ratio of 1:2.5 w/v)  
158 by an Orion 868 pH meter (Thermo Fisher Scientific, Cambridge, Massachusetts, USA)  
159 and salinity (sediment-to-water ratio of 1:5 w/v) by a Eutech Instruments-Salt6 salinity  
160 meter (Thermo Fisher Scientific, San Francisco, California, USA). A subsample was  
161 freeze-dried, homogenized and ground to fine powder, and then sifted through a 2-mm  
162 mesh for measuring sediment total carbon (TC) and total nitrogen (TN) using  
163 Elementar Vario MAX CN analyser (ELEMENTAR, Hanau, Frankfurt, Germany).

164 During each sampling campaign, *in situ* electrical conductivity (EC) and sediment  
165 temperature ( $T_s$ ) were measured by an EC meter (2265FS, Spectrum Technologies,  
166 Aurora, Illinois, USA) and a portable temperature meter (IQ150, IQ Scientific  
167 Instruments, Carlsbad, California, USA), respectively.

168 2.4. *DNA extraction and quantitative PCR*

169 Triplicate sediment samples were collected as aforementioned for quantifying  
170 major N-cycling functional genes. A total of 30 and 90 sediment samples were collected  
171 from the marsh and aquaculture ponds, respectively, over the study period. Total DNA  
172 was extracted from 0.5 g of freeze-dried sediment sample via the FastDNA SPIN Kit

173 for soils (MP Biomedicals, Santa Ana, California, USA) following the manufacturers'  
174 protocols and stored at low temperature ( $-80\text{ }^{\circ}\text{C}$ ). The concentration and quality of  
175 extracted DNA was checked by 1.2% agarose gel electrophoresis and  
176 spectrophotometry (NanoDrop Technologies, Wilmington, North Carolina, USA). The  
177 abundances of N-cycling functional genes were measured on a CFX96 Optical  
178 Real-Time Detection System (Bio-Rad Laboratories Inc., Hercules, CA, USA). The  
179 functional genes we targeted were ones involved in ammonium oxidation (AOA *amoA*,  
180 AOB *amoA*, comammox *Nitrospira* clades A and B *amoA*), nitrite reduction (*nirK*, *nirS*)  
181 and nitrous oxide reduction (*nosZ* I, *nosZ* II). Each reaction mixture (20  $\mu\text{L}$ ) consisted  
182 of 10  $\mu\text{L}$  SYBR mix (Vazyme, Nanjing, China), an optimized concentration of forward  
183 and reverse primers, and 1  $\mu\text{L}$  of template including 1–10 ng of DNA and sterilized  
184 distilled water. A negative control was applied with sterilized distilled water as the  
185 template instead of an extracted DNA sample. The gene-specific primers and thermal  
186 cycling environment are shown in [Table S1](#). Standard curves were produced from a  
187 ten-fold serial dilution of plasmid DNA including the target genes. The amplification  
188 efficiencies were 90–102%, except for comammox *Nitrospira* clade B (79–81%), with  
189  $r^2$  of 0.994 to 0.999 (it should be noted that they were non-specific amplifications for  
190 comammox *Nitrospira* clade B).

### 191 2.5. Production potential of sediment $\text{N}_2\text{O}$

192 Incubation to measure sediment  $\text{N}_2\text{O}$  production potential was conducted according  
193 to [Liu et al. \(2019\)](#) and [Wang et al. \(2017\)](#). Briefly, 50 g (wet weight) of fresh sediment

194 and 50 mL of water collected from each site were added to a 200 mL incubation bottle  
195 and purged with N<sub>2</sub> gas (>99.9999% purity) for 5–8 min to displace the dissolved  
196 oxygen. The bottles were then sealed with a silicone rubber and incubated with  
197 agitation (175 rpm min<sup>-1</sup>) at *in situ* temperature (i.e., sediment temperature measured at  
198 the sampling site; 14–30 °C) for 12 days. A 5-mL gas sample was taken from the  
199 headspace of each incubation bottle with a syringe at the start, then every four days  
200 (total 4 times); 5 mL of N<sub>2</sub> gas was added back each time to keep the pressure. The  
201 extracted gas samples were measured for N<sub>2</sub>O concentrations on a gas chromatograph  
202 (GC-2014, Shimadzu, Japan) equipped with an electron-capture detector (ECD).  
203 Sediment dry weight was measured according to [Yang et al. \(2020b\)](#). Sediment N<sub>2</sub>O  
204 production potential [ng N<sub>2</sub>O g<sup>-1</sup> (dry weight) day<sup>-1</sup>] was calculated from the linear rate  
205 of increase in headspace N<sub>2</sub>O concentration over time ([Liu et al., 2019](#); [Yang et al.,](#)  
206 [2020](#); [Wassmann et al., 1998](#)).

207 Potential denitrification activity was determined according to [Enwall et al. \(2005\)](#)  
208 and [Ma et al. \(2020\)](#) with minor modifications. Briefly, 10 g (wet weight) fresh  
209 sediments were added to a 150 mL incubation bottle and kept at 25 °C overnight. On the  
210 following day, 10 mL of water collected from each site was added to the bottles and  
211 purged with N<sub>2</sub> gas (>99.9999% purity) for 5–8 min to achieve denitrifying conditions.  
212 Acetylene (10% v/v) was added to inhibit the reduction of N<sub>2</sub>O to N<sub>2</sub>. The bottles were  
213 then sealed with a silicone rubber and incubated with agitation (175 rpm min<sup>-1</sup>) at *in*  
214 *situ* temperature for 48 h, and gas samples were collected every 12 h. N<sub>2</sub>O

215 concentrations from gas samples were measured on a gas chromatograph (GC-2014,  
216 Shimadzu, Japan). Sediment potential denitrification activity [ $\text{ng N}_2\text{O g}^{-1}$  (dry weight)  
217  $\text{day}^{-1}$ ] was calculated from the linear rate of increase in headspace  $\text{N}_2\text{O}$  concentration  
218 during the incubation time.

#### 219 *2.6. Measurement of $\text{N}_2\text{O}$ emission fluxes*

220 The  $\text{N}_2\text{O}$  emission fluxes were measured with static closed chambers in the marsh  
221 stand (Marín-Muñiz et al., 2015; Yang et al., 2019) and with floating chambers in the  
222 aquaculture ponds (Chuang et al., 2017; Lorke et al., 2015). The static closed chamber  
223 consisted of a PVC top (100 cm height, 35 cm width, 35 cm length) and a bottom collar  
224 (30 cm height, 35 cm width, 35 cm length); the bottom collar was inserted 20 cm into  
225 the sediment. The floating chamber was made of a plastic basin  
226 (polyethylene/plexiglas®) (Fujian Petrochemical CO., Ltd, Fuzhou, Fujian, China)  
227 (with covering area of  $0.1 \text{ m}^2$  and a volume of 5.2 L) fitted with floating Styrofoam. To  
228 reduce internal heating by sunlight, the floating chamber was covered in reflective tape  
229 (Natchimuthu et al., 2017; Yang et al., 2020). To mix air well inside headspace, an  
230 electric fan was installed inside each chamber.

231 During each sampling campaign, headspace air sample was drawn from each  
232 chamber into an aluminum-foil gas sample bag (Delin Gas Packing Co., Dalian, China)  
233 in 15-minute intervals over a 45 min period. The collected gas samples were returned to  
234 the laboratory for measuring  $\text{N}_2\text{O}$  concentrations within 48 h on the GC-ECD system  
235 mentioned above.  $\text{N}_2\text{O}$  emission fluxes ( $\mu\text{g N}_2\text{O m}^{-2} \text{ h}^{-1}$ ) were calculated as the rate of

236 change in the mass of N<sub>2</sub>O per unit surface area per unit time (Wu et al., 2021; Yuan et  
237 al., 2021).

### 238 2.7. Statistical analysis

239 All data were checked for normality and homogeneity of variance before further  
240 statistical analysis. Differences in environmental parameters, sediment N<sub>2</sub>O production  
241 potential and N<sub>2</sub>O emission fluxes between the marsh and the aquaculture ponds were  
242 tested by using two-way analysis of variance (two-way ANOVA) followed by *Tukey's*  
243 post hoc test, using the SPSS 22.0 (IBM, Armonk, NY, USA). Statistical plots were  
244 generated using OriginPro 2021 (OriginLab Corp. USA). Because N<sub>2</sub>O emission  
245 measurements were done at irregular frequencies over the three-year period (see  
246 Section 2.1), the data were grouped by months for correlation analysis. Spearman  
247 correlation analyses were conducted to analyse the relationships between sediment N<sub>2</sub>O  
248 production potential (or N<sub>2</sub>O emission fluxes), the abundance of various major  
249 N-cycling functional genes and various environmental parameters, using *corrplot* and  
250 *Hmisc* packages in R software (Version 4.1.0). To explore seasonal patterns, the data  
251 were grouped into Spring (from March to May), Summer (from June to August),  
252 Autumn (from September to November) and Winter (from December to February).

253 The main abiotic and biotic variables influencing sediment N<sub>2</sub>O production  
254 potential (or N<sub>2</sub>O emission fluxes) were evaluated by random forest modeling with the  
255 *randomForest* and *rfPermute* packages in R software, and the results were plotted using  
256 OriginPro 2021. The extent to which environmental variables affecting the variability in

257 sediment N<sub>2</sub>O production potential (or N<sub>2</sub>O emission fluxes) was evaluated by using  
258 Redundancy Analysis (RDA) via software CANOCO 5.0 (Microcomputer Power,  
259 Ithaca, New York, USA).

### 260 **3. Results**

#### 261 *3.1. Environmental parameters*

262 The physico-chemical properties of the sediments and porewaters are shown in  
263 [Table 1](#). No significant differences were observed for sediment pH or porewater SO<sub>4</sub><sup>2-</sup>  
264 concentration between the two habitats (ANOVA,  $p > 0.05$ ; [Table 1](#); [Yang et al., 2022c](#)).  
265 However, significant differences were found for the other parameters. Salinity,  $T_s$ , EC  
266 and TN in the marsh sediments were significantly higher while C:N ratio was generally  
267 lower than the pond sediment (ANOVA,  $p < 0.01$ ; [Table 1](#); [Yang et al., 2022c](#)).  
268 Furthermore, porewater NH<sub>4</sub><sup>+</sup>-N and NO<sub>3</sub><sup>-</sup>-N concentrations in the marsh were  
269 significantly larger than in the pond (ANOVA,  $p < 0.01$  or  $< 0.05$ ; [Table 1](#)).

#### 270 *3.2. Functional gene abundance in sediments*

271 The copy numbers of genes for ammonium oxidation (AOA *amoA*, AOB *amoA*  
272 and comammox *Nitrospira amoA*) and denitrification (*nirK*, *nirS*, *nosZ* I, and *nosZ* II)  
273 are shown in [Figure 2](#). No significant differences were found in copy number of the  
274 AOB *amoA* gene between the two habitats ( $p > 0.05$ ; [Figure 2b](#)). However, the copy  
275 number of AOA *amoA* genes in the marsh sediment (mean  $1.9 \times 10^8$  copies g<sup>-1</sup>) was  
276 significantly larger than in the pond sediment ( $7.2 \times 10^6$  copies g<sup>-1</sup>) ( $p < 0.0001$ ; [Figure](#)  
277 [2a](#)). Likewise, the copy numbers of comammox *Nitrospira* clade A and clade B *amoA*

278 genes were significantly higher in the marsh sediment ( $1.8 \times 10^7$  and  $2.2 \times 10^8$  copies  $g^{-1}$ ,  
279 respectively) than in the pond sediment ( $4.1 \times 10^6$  and  $4.7 \times 10^7$  copies  $g^{-1}$ , respectively)  
280 ( $p < 0.001$ ; [Figures 2c and 2d](#)). The mean copy numbers of the *nirK*, *nirS*, *nosZ* I and  
281 *nosZ* II genes in the marsh sediment ( $1.5 \times 10^8$ ,  $5.9 \times 10^8$ ,  $2.9 \times 10^8$  and  $3.0 \times 10^8$  copies  $g^{-1}$ ,  
282 respectively) were all significantly larger than those in the pond sediment ( $2.8 \times 10^7$ ,  
283  $1.8 \times 10^8$ ,  $1.1 \times 10^8$  and  $2.7 \times 10^7$  copies  $g^{-1}$ , respectively) ( $p < 0.001$ ; [Figures 2e-2h](#)).

### 284 3.3. Sediment $N_2O$ production potentials

285 The monthly sediment  $N_2O$  production potential changed in the range of 47.9–65.4  
286  $ng\ g^{-1}\ d^{-1}$  in the marsh and in the range of 37.5–47.9  $ng\ g^{-1}\ d^{-1}$  in the aquaculture ponds  
287 ([Figure 3a](#)). The mean value in the marsh sediment ( $53.9 \pm 1.5\ ng\ g^{-1}\ d^{-1}$ ) was  
288 significantly larger than that in the aquaculture pond sediment ( $42.1 \pm 1.1\ ng\ g^{-1}\ d^{-1}$ )  
289 ( $F_{df=1}=56.630$ ,  $p < 0.0001$ ; [Figure 4a](#)). Seasonally, the highest sediment  $N_2O$  production  
290 potential occurred during the spring in the marsh, and during the summer in the  
291 aquaculture ponds ([Figure 3b](#)). In addition, we observed that the mean sediment  
292 potential denitrification activity in the marsh ( $92.9 \pm 8.6\ ng\ g^{-1}\ d^{-1}$ ) was significantly  
293 higher than that in the aquaculture pond sediment ( $54.6 \pm 3.3\ ng\ g^{-1}\ d^{-1}$ ) ( $F_{df=1}=17.274$ ,  
294  $p < 0.001$ ; [Figure S1](#)).

### 295 3.4. $N_2O$ emission fluxes

296  $N_2O$  emission fluxes changed significantly during the study period ( $p < 0.01$ ),  
297 ranging from  $12.6 \pm 0.6$  to  $570.7 \pm 14.2\ \mu g\ m^{-2}\ h^{-1}$  in the marsh, and  $5.4 \pm 0.9$  to  
298  $251.8 \pm 160.9\ \mu g\ m^{-2}\ h^{-1}$  in the aquaculture ponds ([Figure 5a](#)). The mean flux from the

299 marsh ( $173.7 \pm 24.2 \mu\text{g m}^{-2} \text{h}^{-1}$ ) was significantly larger than that from the aquaculture  
300 ponds ( $42.9 \pm 9.5 \mu\text{g m}^{-2} \text{h}^{-1}$ ) ( $F_{df=1}=25.373, p < 0.0001$ ; [Figure 4b](#)). By grouping the data,  
301 a seasonal pattern emerged, with lower emission fluxes in autumn and winter, and  
302 higher fluxes in spring and summer, in both habitat types ([Figure 5b and 5c](#)).

### 303 3.5. Environmental drivers of $\text{N}_2\text{O}$ productions and fluxes

304 The correlations between sediment  $\text{N}_2\text{O}$  production potential and  $\text{N}_2\text{O}$  emission  
305 flux and the different biotic and abiotic variables are shown in [Figure 6](#). Based on  
306 Pearson correlations ([Figure 6](#)) and RFP analysis ([Figure 7](#)), the changes in  $\text{N}_2\text{O}$   
307 emission flux were strongly driven by *nirK* gene abundance, N substrate concentrations  
308 (e.g., TN,  $\text{NO}_3^-$ -N and  $\text{NH}_4^+$ -N) and  $T_s$ , which together explained nearly 55% of the  
309 variations.

310 Based on RDA, sediment salinity, C:N ratio, TN and porewater  $\text{NH}_4^+$ -N  
311 concentration were the main variables explaining the changes of sediment  $\text{N}_2\text{O}$   
312 production potential and  $\text{N}_2\text{O}$  emission fluxes in marsh. In particular, C:N accounted  
313 for the largest contribution ([Figure S2a](#)). In the aquaculture ponds, sediment  $\text{N}_2\text{O}$   
314 production potential and  $\text{N}_2\text{O}$  emission fluxes were strongly driven by  $T_s$  and C:N ratio,  
315 which together explained nearly 83% of the changes ([Figure S2b](#)).

## 316 4. Discussion

317 Large increases in  $\text{N}_2\text{O}$  and  $\text{CH}_4$  emissions following conversion of natural  
318 wetlands to agriculture systems (e.g., croplands, pastures), which have also been  
319 reported by other scholars (e.g., [Gleason et al., 2009](#); [Huang et al., 2010](#); [Tan et al.,](#)

320 [2019; Olsson et al., 2015](#)), are usually attributed to the increase in precursor substrates  
321 and changes in soil properties ([Tan et al., 2019](#)). For aquaculture ponds, application of  
322 fertilizer, organic loading from feeds and farmed animals, and oxygen depletion in  
323 waterlogged sediment are all expected to promote N<sub>2</sub>O production and emission ([Hu et](#)  
324 [al., 2012; Mosier et al., 1991; Tan et al., 2020](#)). In China and elsewhere in the  
325 Asia-Pacific region, conversion of natural wetlands to aquaculture ponds is widespread  
326 to satisfy the growing food demand, raising concerns about their climate impact ([Yuan](#)  
327 [et al., 2019; Stokal et al., 2021](#)). By comparing the brackish marsh and the converted  
328 aquaculture ponds within the Shanyutan wetland, Southeast China, this study examined  
329 the effect of LULCC on sediment properties and related N<sub>2</sub>O production and emission.

#### 330 *4.1. Effects of land use change on sediment N-cycling microbes*

331 Other scholars have shown that the abundance of major N-cycling functional  
332 genes in sediments are positively affected by N substrate availability ([Bahram et al.,](#)  
333 [2022; Gao et al., 2019; Sun et al., 2021](#)). Likewise, in this study, variations in the  
334 abundance of major N-cycling functional genes in the sediment samples were  
335 correlated positively to N substrates ([Figure 6](#)) and negatively to C:N ratio ([Figure 6](#)),  
336 confirming N substrate availability as a key factor regulating the sediment microbial  
337 community and its N cycling ability in coastal wetlands. Contrary to expectations that  
338 aquaculture would increase nitrogen loading to the sediment ([Das et al., 2004; Burford](#)  
339 [and Lorenzen, 2004](#)), we found that marsh actually had higher sediment TN and  
340 porewater inorganic nitrogen concentrations than pond ([Table 1](#)), likely a result of N

341 release from marsh vegetation and high N input from the catchment (Li et al., 2021b).  
342 Accordingly, the abundance of the nitrifying functional genes (AOA and comammox  
343 *Nitrospira amoA*) and denitrifying functional genes (e.g., *nirK*, *nirS*, *nosZ* I and *nosZ* II)  
344 in the marsh sediment were significantly more abundant than in the pond sediment  
345 (Figure 2), suggesting that land conversion of natural marsh to aquaculture ponds  
346 negatively impacted sediment N substrate (i.e., TN,  $\text{NH}_4^+$ -N and  $\text{NO}_3^-$ -N) availability  
347 and the corresponding sediment N-cycling ability. Moreover, comammox *Nitrospira*  
348 *amoA* were positively correlated with  $\text{NO}_3^-$ -N and negatively impacted by land use  
349 change, suggesting that the newly discovered nitrifying microorganisms might play an  
350 important role in sediment nitrification but were diminished during the conversion of  
351 natural marsh to aquaculture ponds.

#### 352 4.2. Effects of land use change on sediment $\text{N}_2\text{O}$ production

353 Sediment  $\text{N}_2\text{O}$  production potential decreased by 22% between coastal marsh and  
354 aquaculture ponds (Figure 4a), suggesting that land conversion may have weakened the  
355 sediment's ability to produce  $\text{N}_2\text{O}$ . The sediment N cycle involves a series of aerobic  
356 (e.g., nitrification) and anaerobic (e.g., denitrification) microbial reactions, with  $\text{N}_2\text{O}$  as  
357 one of the intermediate products (Daims et al., 2016; Li et al., 2021a). In this study, the  
358 variations in sediment  $\text{N}_2\text{O}$  production potential were positively correlated to N  
359 substrates, as well as the different N-cycling functional genes (Figure 6), including the  
360 ones involved in ammonium oxidation (AOA and comammox *Nitrospira amoA*), nitrite  
361 reduction (*nirK* and *nirS*) and nitrous oxide reduction (*nosZ* I and *nosZ* II). Both

362 ammonium oxidation and nitrite reduction are steps in converting fixed N to N<sub>2</sub>O,  
363 whereas nitrous oxide reduction converts NO to N<sub>2</sub>O and further to N<sub>2</sub>; therefore, the  
364 net production of N<sub>2</sub>O in the sediment depends on the balance between microbial  
365 formation and consumption of N<sub>2</sub>O. Our data suggest that the microbial processes of  
366 N<sub>2</sub>O formation outpaced N<sub>2</sub>O consumption, leading to a net positive N<sub>2</sub>O production  
367 potential in the sediment. In marsh sediment, the strong correlations between N<sub>2</sub>O  
368 production potential and abundance of the AOA *amoA* gene (Figure S3a) and the *nirK*  
369 gene (Figure S3c) showed that ammonium oxidizing archaea and denitrifying bacteria  
370 were the key members of the microbial community to drive N<sub>2</sub>O production in coastal  
371 wetland. Conversely, land conversion to aquaculture ponds appeared to have negatively  
372 impacted the populations of ammonium oxidizing archaea and denitrifying bacteria  
373 (Figure 2a,c), which, combined with the lower N substrate availability, likely explained  
374 the smaller sediment N<sub>2</sub>O production potential in the aquaculture ponds (Figure 4a).

#### 375 4.3. Effects of land use change on N<sub>2</sub>O emission flux

376 N<sub>2</sub>O emission in the brackish marsh correlated strongly and negatively with  
377 sediment salinity (Table S2). Sediment salinity in the brackish marsh might vary due to  
378 tidal flushing and river runoff, causing stress to the microbial community (Francis et al.,  
379 2003). N<sub>2</sub>O emission flux was largest in the spring in coastal marsh (Figure 5b),  
380 perhaps reflecting the effect of N-substrates from decomposing biomass from the  
381 preceding winter (Jiang et al., 2009; Sommerfeld et al., 1993).

382 The aquaculture ponds were isolated from tides and river runoff and therefore

383 sediment salinity variation was a less important factor. N<sub>2</sub>O emission was highest in the  
384 summer (Figure 5c), which was the beginning of the culture period, and adding feeds  
385 and farmed animals would have increased N substrate availability for N<sub>2</sub>O production  
386 (positive correlation; Table S2). The stagnant nature of pond water would have also  
387 allowed sediment temperature to increase in hot months (summer), causing increased  
388 microbial N<sub>2</sub>O production (positive correlation; Table S2) and decreased N<sub>2</sub>O solubility,  
389 consistent with the higher N<sub>2</sub>O emission flux in the summer (Figure 5c).

390 Our data showed that overall, the marsh sediment had higher N substrate  
391 concentrations, abundances of major N-cycling functional genes and sediment N<sub>2</sub>O  
392 production potential, all expected to drive higher N<sub>2</sub>O emission in the marsh than in the  
393 aquaculture ponds, according to the correlation analysis results (Figure 6). Indeed,  
394 except for the months of July and August in 2019, N<sub>2</sub>O emission fluxes in coastal  
395 marsh were consistently higher than in aquaculture ponds throughout the three-year  
396 period, sometimes by as much as 8-fold (Figure 5a). Averaging the entire data set, N<sub>2</sub>O  
397 emission from the marsh was 4 times that from the aquaculture ponds (Figure 4b).

398 In addition, we calculated the indirect N<sub>2</sub>O emission factor (EF<sub>5</sub>) for the two  
399 habitat types following the N<sub>2</sub>O–N/NO<sub>3</sub><sup>-</sup>–N mass ratio methodology (Hama-Aziz et al.,  
400 2017; Turner et al. 2015). We found that the mean EF<sub>5</sub> value in the brackish marsh  
401 (0.0008) was greater than that in the aquaculture ponds (0.0003) by over 2.6 times,  
402 further demonstrating that the marsh was a stronger N<sub>2</sub>O source even at the same level  
403 of N supply. Overall, the EF<sub>5</sub> values in our two habitats were found to be lower than the

404 IPCC default value of 0.0025 for rivers and estuaries (De Klein et al. 2006), but  
405 comparable to those in other inland waters (e.g., Audet et al., 2017; Cooper et al., 2017;  
406 Outram and Hiscock, 2012; Qin et al., 2019; Tian et al., 2018) and estuaries (Maavara  
407 et al., 2019; Qi et al., 2022), and even higher than those in rivers (Maavara et al., 2019).  
408 Hence, the N<sub>2</sub>O emissions from brackish marshes and aquaculture ponds **should** not be  
409 overlooked in accounting for the global sources of N<sub>2</sub>O.

#### 410 *4.4 Long-term land use change effects in the local context*

411 Coastal and freshwater wetlands not only perform important ecosystem services,  
412 but they are also major carbon sinks (Chmura et al., 2003; Mitsch et al., 2013). As such,  
413 reclamation of wetlands especially for farming purposes is expected to increase nutrient  
414 and organic loading to the systems, compromise their carbon sequestration capacity,  
415 and increase the overall production and emission of greenhouse gases including CH<sub>4</sub>  
416 and N<sub>2</sub>O. This appears to be true on a global scale (Tan et al., 2019). However, at the  
417 local scale, the effect of LULCC may depend on changes to the local hydrology,  
418 nutrient dynamics and microbial communities, which need to be assessed by detailed  
419 comparisons between the original and the converted habitats.

420 Our high-frequency measurements over a three-year period showed that the  
421 aquaculture ponds in the Shanyutan wetland had lower N<sub>2</sub>O emission than the native  
422 brackish marsh, which was supported by independent measurements of the lower  
423 N-substrate concentrations, lower major N-cycling functional gene abundances and  
424 lower sediment N<sub>2</sub>O production potential in the pond sediment. In the aquaculture

425 ponds, exogenous N supply in the form of feeds was one of the major sources of N  
426 substrates for N<sub>2</sub>O production. In our study, the rate of N input via feed application was  
427 approximately 28.5 g N m<sup>-2</sup> year<sup>-1</sup>. Meanwhile, the average N<sub>2</sub>O emission from the  
428 aquaculture ponds was only 0.14 g N m<sup>-2</sup> year<sup>-1</sup>, accounting for about 0.5% of the total  
429 annual N loading arising from feed inputs. Over 40% of the added N was actually  
430 incorporated into the biomass of the cultured whiteleg shrimps (*Litopenaeus vannamei*),  
431 which had a relatively high nutrient utilization efficiency (Yang et al., 2021). We found  
432 that our pond sediments had a mean denitrification potential and net N<sub>2</sub>O production  
433 potential of 54.6 and 42.1 ng g<sup>-1</sup> d<sup>-1</sup>, respectively, which implied that 23% of the N<sub>2</sub>O  
434 produced was further converted to N<sub>2</sub> gas. Hence, our results suggested that shrimp  
435 biomass incorporation and sediment N storage were likely major fates of the N applied  
436 in the ponds, while gaseous loss of N was minimal.

437 In the brackish marshes, the sediments can receive N supply from both surface  
438 water and atmospheric deposition for supporting N<sub>2</sub>O production. In our study, we  
439 observed a significantly higher amount of total nitrogen (TN) in the marsh sediments  
440 than that in the aquaculture pond sediments (1.34 vs. 0.70 g kg<sup>-1</sup>), implying a  
441 substantially greater amount of external N inputs into the marsh as compared to the  
442 ponds. Owing to the greater N availability, the brackish marshes had a significantly  
443 greater potential denitrification rate than the brackish marshes (92.9 vs. 54.6 ng g<sup>-1</sup> d<sup>-1</sup>).  
444 Meanwhile, the potential N<sub>2</sub> production rate of denitrification was also much higher in  
445 the marshes than in the ponds (39.0 vs. 12.5 ng g<sup>-1</sup> d<sup>-1</sup>), with about 42% of the N<sub>2</sub>O

446 produced in the marsh sediments being subsequently reduced. As a result, the brackish  
447 marsh sediments still had higher mean N<sub>2</sub>O production potential (53.9 vs. 42.8 ng g<sup>-1</sup> d<sup>-1</sup>)  
448 and net N<sub>2</sub>O emission rate (173.7 vs. 42.9 μg m<sup>-2</sup> h<sup>-1</sup>), when compared to the pond  
449 sediments.

450 Taken together, we suggest that conversion of the Shanyutan brackish marsh to  
451 aquaculture ponds cut off N loading from the catchment and marsh vegetation that  
452 fueled N<sub>2</sub>O production. Of the residual N that entered the sediment, its conversion to  
453 N<sub>2</sub>O would still require a series of microbial processes. As our data showed, the major  
454 N-cycling functional gene abundances in the pond sediment were all significantly lower,  
455 except the AOB *amoA* (Figure 2), suggesting that the marsh sediment microbial  
456 community was negatively impacted by land reclamation, leading to a much lower  
457 ability to produce N<sub>2</sub>O (Figure 4a) and correspondingly a lower N<sub>2</sub>O emission (Figure  
458 4b). These findings are also consistent with an earlier study which, using a mass  
459 balance approach, showed that N<sub>2</sub>O emission accounted for ≤ 0.03 % of the total N  
460 output from the aquaculture ponds (Yang et al., 2021).

461 Microbial production of N<sub>2</sub>O can follow both aerobic and anaerobic pathways  
462 (Baggs, 2011; Yang et al., 2015). In this study, we incubated sediment slurry under  
463 anoxic condition and therefore, we may have underestimated the sediment N<sub>2</sub>O  
464 production potential by excluding the aerobic processes, although this would not have  
465 affected the functional gene abundance and emission flux measurements. Quantification  
466 of N<sub>2</sub>O production *in situ* using novel tracer method (Yeung et al., 2019) would

467 eliminate the need for incubation and generate more accurate data. Another interesting  
468 observation is the large between-month and between-year variations in N<sub>2</sub>O emission in  
469 the marsh (Figure 5); measurements at a lower frequency or measurements that cover a  
470 shorter period may lead to considerable errors in the N<sub>2</sub>O emission budget.

471 After harvesting, shrimp farmers usually drain the ponds and dry the sediment.  
472 This process, while may release residual N into the estuary and increase N<sub>2</sub>O  
473 production and emission downstream, would not be inducive to microbial N<sub>2</sub>O  
474 production in the pond sediment during the non-farming period. Nevertheless,  
475 post-harvesting removal of sediment is not a common practice; therefore, continuous  
476 build-up of N in the pond sediment may pose the risk of a future surge in N<sub>2</sub>O emission.  
477 Preventive measures to better manage N discharge and sediment build-up would be  
478 needed to further mitigate N<sub>2</sub>O emission caused by the aquaculture operation.

## 479 **5. Conclusions**

480 Overall, our findings highlighted the importance of local context for understanding  
481 LULCC effects on greenhouse gas dynamics. While it may be tempting to presume that  
482 reclamation of natural wetlands to aquaculture ponds would increase N<sub>2</sub>O emission, our  
483 multi-year field study showed the opposite. Nevertheless, our sampling was limited to  
484 the Shanyutan wetland and one type of aquaculture operation, whereas other wetlands  
485 and aquaculture systems may have different environmental conditions and microbial  
486 communities, possibly resulting in different N<sub>2</sub>O dynamics. Reclamation of coastal  
487 wetlands for aquaculture is widespread throughout the southeastern coast of China,

488 from the tropical zone to the subtropical zone (Duan et al. 2020). Expanding the  
489 sampling efforts to the other regions would be needed for a fuller understanding of the  
490 LULCC effects on coastal greenhouse gas dynamics in this aquaculture-intensive  
491 country.

## 492 **Declaration of competing interest**

493 The authors declare that they have no known competing financial interests or  
494 personal relationships that could have appeared to influence the work reported in this  
495 paper.

## 496 **Acknowledgements**

497 This research was supported by the National Natural Science Foundation of China  
498 (NSFC) (Grant No. 41801070, and No. 41671088), the National Natural Science  
499 Foundation of Fujian Province (Grant No. 2020J01136), and the Minjiang Scholar  
500 Programme.

## 501 **References**

- 502 Audet, J., Wallin, M.B., Kyllmar, K., Andersson, S., Bishop, K., 2017. Nitrous oxide  
503 emissions from streams in a Swedish agricultural catchment. *Agr. Ecosyst. Environ.*  
504 236, 295–303. <https://doi.org/10.1016/j.agee.2016.12.012>
- 505 Bahram, M., Espenberg, M., Pärn, J., Lehtovirta-Morley, L., Anslan, S., Kasak, K.,  
506 Kõljalg, U., Liira, J., Maddison, M., Moora, M., Niinemets, Ü., Öpik, M., Pärtel, M.,  
507 Soosaar, K., Zobel, M., Hildebrand, F., Tedersoo, L., Mander, Ü., 2022. Structure  
508 and function of the soil microbiome underlying N<sub>2</sub>O emissions from global  
509 wetlands. *Nat. Commun.* 3, 1430. <https://doi.org/10.1038/s41467-022-29161-3>

510 Baggs, E.M., 2011. Soil microbial sources of nitrous oxide: recent advances in  
511 knowledge, emerging challenges and future direction. *Curr. Opin. Environ. Sust.*  
512 3(5), 321–327. <https://doi.org/10.1016/j.cosust.2011.08.011>

513 Batjes, N.H. 1996. Total carbon and nitrogen in the soils of the world. *Eur. J. Soil Sci.*,  
514 47, 151–163. <https://doi.org/10.1111/ejss.12115>

515 Burford, M. A., Lorenzen, K. (2004). Modeling nitrogen dynamics in intensive shrimp  
516 ponds: the role of sediment remineralization. *Aquaculture*, 229(1-4), 129-145.  
517 [https://doi.org/10.1016/S0044-8486\(03\)00358-2](https://doi.org/10.1016/S0044-8486(03)00358-2)

518 Chmura, G.L., Anisfeld, S.C., Cahoon, D.R., Lynch, J.C., 2003. Global carbon  
519 sequestration in tidal, saline wetland soils. *Glob. Biogeochem. Cycles* 17 (4), 1111.  
520 <https://doi.org/10.1029/2002GB001917>

521 Chuang, P.-C., Young, M.B., Dale, A.W., Miller, L.G., Herrera-Silveira, J.A., Paytan, A.,  
522 2017. Methane fluxes from tropical coastal lagoons surrounded by mangroves,  
523 Yucatán, Mexico. *J. Geophys. Res. Biogeosci.* 122 (5), 1156–1174.  
524 <https://doi.org/10.1002/2017JG003761>

525 Cooper, R.J., Wexler, S.K., Adams, C.A., Hiscock, K.M., 2017. Hydrogeological  
526 controls on regional-scale indirect nitrous oxide emission factors for rivers. *Environ.*  
527 *Sci. Technol.* 51, 10440–10448. <https://doi.org/10.1021/acs.est.7b02135>

528 Daims, H., Lücker, S., Wagner, M., 2016. A new perspective on microbes formerly  
529 known as nitrite-oxidizing bacteria. *Trends Microbiol.* 24(9), 699–712.  
530 <https://doi.org/10.1016/j.tim.2016.05.004>

531 Das, B., Khan, Y.S. A., Das, P., 2004. Environmental impact of  
532 aquaculture-sedimentation and nutrient loadings from shrimp culture of the  
533 southeast coastal region of the Bay of Bengal. *J. Environ. Sci.* 16(3), 466-470.  
534 <https://doi.org/10.3321/j.issn:1001-0742.2004.03.025>

535 Duan, Y.Q., Li, X., Zhang, L.P., Chen, D., Liu, S.A., Ji, H.Y., 2020. Mapping  
536 national-scale aquaculture ponds based on the Google Earth Engine in the Chinese  
537 coastal zone. *Aquaculture* 520, 734666.  
538 <https://doi.org/10.1016/j.aquaculture.2019.734666>

539 Enwall, K., Philippot, L., Hallin, S., 2005. Activity and composition of the denitrifying  
540 bacterial community respond differently to long-term fertilization. *Appl. Environ.*

541 Microbiol. 71, 8335–8343. <https://doi.org/10.1128/AEM.71.12.8335-8343.2005>

542 FAO, 2020. The state of world fisheries and aquaculture 2020. Sustainability in Action,  
543 Rome. <https://doi.org/10.4060/ca9229en>

544 Francis, C.A., O’Mullan, G.D., Ward, B.B., 2003. Diversity of ammonia  
545 monooxygenase (*amoA*) genes across environmental gradients in Chesapeake Bay  
546 sediments. Geobiology 1, 129-140  
547 <https://doi.org/10.1046/j.1472-4669.2003.00010.x>

548 Gao, D.Z., Liu, M., Hou, L.J., Lai D.Y.F., Wang, W.Q., Li, X.F., Zeng, A.Y., Zheng,  
549 Y.L., Han, P., Yang, Y., Yin, G.Y., 2019. Effects of shrimp-aquaculture reclamation  
550 on sediment nitrate dissimilatory reduction processes in a coastal wetland of  
551 southeastern China. Environ. Pollut. 255, 113219.  
552 <https://doi.org/10.1016/j.envpol.2019.113219>

553 Gleason, R.A., Tangen, B.A., Browne, B.A., Euliss Jr. N.H., 2009. Greenhouse gas flux  
554 from cropland and restored wetlands in the Prairie Pothole Region. Soil Biol.  
555 Biochem. 41, 2501–2507. <https://doi.org/10.1016/j.soilbio.2009.09.008>

556 Gutlein, A., Gerschlauser, F., Kikoti, I., Kiese, R., 2018. Impacts of climate and land use  
557 on N<sub>2</sub>O and CH<sub>4</sub> fluxes from tropical ecosystems in the Mt. Kilimanjaro region,  
558 Tanzania. Glob. Change Biol. 24, 1239–1255. <https://doi.org/10.1111/gcb.13944>

559 Hama-Aziz, Z.Q., Hiscock, K.M., Cooper, R.J., 2017. Indirect nitrous oxide emission  
560 factors for agricultural field drains and headwater streams. Environ. Sci. Technol.  
561 51, 301–307. <https://doi.org/10.1021/acs.est.6b05094>

562 He, G.S., Wang, K.Y., Zhong, Q.C., Zhang, G.L., van den Bosch, C.K., Wang, J.T.,  
563 2021. Agroforestry reclamations decreased the CO<sub>2</sub> budget of a coastal wetland in  
564 the Yangtze estuary. Agr. Ecosyst. Environ. 296, 108212.  
565 <https://doi.org/10.1016/j.agrformet.2020.108212>

566 Herbeck, L.S., Unger, D., Wu, Y., Jennerjahn, T.C., 2013. Effluent, nutrient and organic  
567 matter export from shrimp and fish ponds causing eutrophication in coastal and  
568 back-reef waters of NE Hainan, tropical China. Cont. Shelf Res. 57, 92–104.  
569 <http://dx.doi.org/10.1016/j.csr.2012.05.006>.

570 Hu, Z., Lee, J.W., Chandran, K., Kim, S., Khanal, S.K., 2012. Nitrous oxide (N<sub>2</sub>O)  
571 emission from aquaculture: a review. Environ. Sci. Technol. 46, 6470–6480.

572 <https://doi.org/10.1021/es300110x>

573 Huang, Y., Sun, W.J., Zhang, W., Yu, Y.Q., Su, Y.H., Song, C.C., 2010. Marshland  
574 conversion to cropland in northeast China from 1950 to 2000 reduced the  
575 greenhouse effect. *Glob. Change Biol.* 16, 680–695.  
576 <https://doi.org/10.1111/j.1365-2486.2009.01976.x>

577 IPCC, 2013. In: Stocker, T.F., Qin, D., Plattner, G.K., Tignor, M., Allen, S.K.,  
578 Boschung, J., Nauels, A., Xia, Y., Bex, V., Midgley, P.M. (Eds.), *Climate Change*  
579 *2013: The Physical Science Basis. Contribution of Working Group I to the Fifth*  
580 *Assessment Report of the Intergovernmental Panel on Climate Change.* Cambridge  
581 University Press, Cambridge, United Kingdom and New York, NY, USA, pp. 1535.

582 Jiang, C.S., Wang, Y.S., Hao, Q.J., Song, C.C., 2009. Effect of land-use change on CH<sub>4</sub>  
583 and N<sub>2</sub>O emissions from freshwater marsh in Northeast China. *Atmos. Environ.* 43,  
584 3305–3309. <https://doi.org/10.1016/j.atmosenv.2009.04.020>

585 Kongkeo, H., 1997. Comparison of intensive shrimp farming systems in Indonesia,  
586 Philippines. Taiwan Thailand. *Aquac. Res.* 28, 789–796.  
587 <http://dx.doi.org/10.1046/j.1365-2109.1997.00943.x>

588 Li, S. H., Zhou, X., Cao, X. W., & Chen, J. B. 2021a. Insights into simultaneous  
589 anammox and denitrification system with short-term pyridine exposure: Process  
590 capability, inhibition kinetics and metabolic pathways. *Front. Environ. Sci. Eng.* 15.  
591 <https://doi.org/10.1007/s11783-021-1433-3>

592 Li, X.F., Qian, W., Hou, L.J., Liu, M., Chen, Z.B., Tong, C., 2021b. Human activity  
593 intensity controls the relative importance of denitrification and anaerobic  
594 ammonium oxidation across subtropical estuaries. *Catena* 202, 105260.  
595 <https://doi.org/10.1016/j.catena.2021.105260>

596 Liu, J.G., Hartmann, S.C., Keppler, F., Lai, D.Y.F., 2019. Simultaneous abiotic  
597 production of greenhouse gases (CO<sub>2</sub>, CH<sub>4</sub>, and N<sub>2</sub>O) in Subtropical Soils. *J.*  
598 *Geophys. Res.-Biogeo.* 124(7), 1977–1987. <https://doi.org/10.1029/2019JG005154>

599 Lorke, A., Bodmer, P., Noss, C., Alshboul, Z., Koschorreck, M., Somlai-Haase, C.,  
600 Bastviken, D., Flury, S., McGinnis, D.F., Maeck, A., Müller, D., Premke, K., 2015.  
601 Technical note: drifting versus anchored flux chambers for measuring greenhouse  
602 gas emissions from running waters. *Biogeosciences* 12 (23), 7013–7024.

603 <https://doi.org/10.5194/bg-12-7013-2015>

604 Ma, L., Jiang, X.L., Liu, G.H., Yao, L.G., Liu, W.Z., Pan, Y.T., Zuo, Y.X., 2020.  
605 Environmental factors and microbial diversity and abundance jointly regulate soil  
606 nitrogen and carbon biogeochemical processes in Tibetan wetlands. *Environ. Sci.*  
607 *Technol.* 54, 3267–3277. <https://doi.org/10.1021/acs.est.9b06716>

608 Marín-Muñiz, J.L., Hernández, M.E., Moreno-Casasola, P., 2015. Greenhouse gas  
609 emissions from coastal freshwater wetlands in Veracruz Mexico: effect of plant  
610 community and seasonal dynamics. *Atmos. Environ.* 107, 107–117.  
611 <https://doi.org/10.1016/j.atmosenv.2015.02.036>

612 Matos, C.R.L., Mendoza, U., Diaz, R., Moreira, M., Belem, A.L., Metzger, E.,  
613 Albuquerque, A.L.S., Machado, W., 2016. Nutrient regeneration susceptibility  
614 under contrasting sedimentary conditions from the Rio de Janeiro coast, Brazil. *Mar.*  
615 *Pollut. Bull.* 108(1-2), 297–302. <https://doi.org/10.1016/j.marpolbul.2016.04.046>

616 Mitsch, W.J., Bernal, B., Nahlik, A.M., Mander, Ü., Zhang, L.I., Anderson, C.J.,  
617 Jørgensen, S.E., Brix, H., 2013. Wetlands, carbon, and climate change. *Landscape*  
618 *Ecol.* 28, 583–597. <https://doi.org/10.1007/s10980-012-9758-8>

619 Mosier, A., Schimel, D., Valentine, D., Bronson, K., Parton, W., 1991. Methane and  
620 nitrous oxide fluxes in native, fertilized and cultivated grasslands. *Nature* 350, 330–  
621 332. <https://doi.org/10.1038/350330a0>

622 Murray, N.J., Phinn, S.R., DeWitt, M., Ferrari, R., Johnston, R., Lyons, M.B., Fuller,  
623 R.A., 2019. The global distribution and trajectory of tidal flats. *Nature* 565, 222–  
624 225. <https://doi.org/10.1038/s41586-018-0805-8>

625 Natchimuthu, S., Sundgren, I., Gålfalk, M., Klemedtsson, L., Bastviken, D., 2017.  
626 Spatiotemporal variability of lake  $p\text{CO}_2$  and  $\text{CO}_2$  fluxes in a hemiboreal catchment.  
627 *J. Geophys. Res. Biogeosci.* 122, 30–49. <https://doi.org/10.1002/2016JG003449>

628 Neubauer, S.C., Megonigal, J.P., 2015. Moving beyond global warming potentials to  
629 quantify the climatic role of ecosystems. *Ecosystems* 18(6), 1000–1013.  
630 <https://doi.org/10.1007/s10021-015-9879-4>

631 Olsson, L., Ye, S., Yu, X., Wei, M., Krauss, K.W., Brix, H., 2015. Factors influencing  
632  $\text{CO}_2$  and  $\text{CH}_4$  emissions from coastal wetlands in the Liaohe Delta, Northeast China.  
633 *Biogeosciences*, 12, 4965–4977. <https://doi.org/10.5194/bg-12-4965-2015>

- 634 Ravishankara, A.R., Daniel, J.S., Portmann, R.W., 2009. Nitrous oxide (N<sub>2</sub>O): the  
635 dominant ozone-depleting substance emitted in the 21st century. *Science* 326, 123–  
636 125. <https://doi.org/10.1126/science.1176985>
- 637 Roulet, N.T., 2000. Peatlands, carbon storage, greenhouse gases, and the Kyoto  
638 Protocol: prospects and significance for Canada. *Wetlands* 20(4), 605–615.
- 639 Shaaban, M., Wu, Y.P., Khalid, M.S., Peng, Q.A., Xu, X.Y., Wu, L., Younas, A., Bashir,  
640 S., Mo, Y.L., Lin, S., Zafar-ul-Hye, M., Abid, M., Hu, R.G., 2018. Reduction in soil  
641 N<sub>2</sub>O emissions by pH manipulation and enhanced *nosZ* gene transcription under  
642 different water regimes. *Environ. Pollut.* 235, 625–631.  
643 <https://doi.org/10.1016/j.envpol.2017.12.066>
- 644 Sommerfeld, R.A., Mosier, A.R., Musselman, R.C., 1993. CO<sub>2</sub>, CH<sub>4</sub> and N<sub>2</sub>O flux  
645 through a Wyoming snowpack and implications for global budgets. *Nature*  
646 361(6408), 140–142. <https://doi.org/10.1038/361140a0>
- 647 Strack, M., Waddington, J.M., 2008. Spatiotemporal variability in peatland subsurface  
648 methane dynamics. *J. Geophys. Res.-Biogeo.* 113(G2), G02010.  
649 <https://doi.org/10.1029/2007JG000472>
- 650 Stokal, M., Janssen, A.B.G., Chen, X., Kroeze, C., Li, F., Ma, L., Yu, H., Zhang, F.,  
651 Wang, M., 2021. Green agriculture and blue water in China: reintegrating crop and  
652 livestock production for clean water. *Front. Agric. Sci. Eng.* 8(1), 72-80.  
653 <https://doi.org/10.15302/J-FASE-2020366>
- 654 Sun, Z.G., Sun, W.G., Tong, C., Zeng, C.S., Yu, X., Mou, X.J., 2015. China's coastal  
655 wetlands: Conservation history, implementation efforts, existing issues and  
656 strategies for future improvement. *Environ. Int.* 79, 25–41.  
657 <http://dx.doi.org/10.1016/j.envint.2015.02.017>
- 658 Sun, D.Y., Liu, M., Hou, L.J., Zhao, M.Y., Tang, X.F., Zhao, Q., Li, J., Han, P., 2021.  
659 Community structure and abundance of comammox *Nitrospira* in Chongming  
660 eastern intertidal sediments. *J. Soil. Sediment.* 21, 3213–3224.  
661 <https://doi.org/10.1007/s11368-021-02940-z>
- 662 Pouil, S., Samsudin, R., Slembrouck, J., Sihabuddin, A., Sundari, G., Khazaidan, K.,  
663 Kristanto, A.H., Pantjara, B., Caruso, D., 2019. Nutrient budgets in a small-scale  
664 freshwater fish pond system in Indonesia. *Aquaculture* 504, 267–274.

665 <https://doi.org/10.1016/j.aquaculture.2019.01.067>

666 Qi, M.T., Luo, L., Hong, X.J., Qian, W., Tong, C., Li, X.F., 2022. Spatial and temporal  
667 variations and influencing factors of nitrous oxide emissions from surface water in  
668 Min River Estuary. *Acta Scientiae Circumstantiae* 42(7), 489–500 (in Chinese).  
669 <https://doi.org/10.13671/j.hjkxxb.2022.0134>

670 Qin, X.B., Li, Y., Goldberg, S., Wan, Y.F., Fan, M.R., Liao, Y.L., Wang, B., Gao, Q.Z.,  
671 Li, Y.E., 2019. Assessment of indirect N<sub>2</sub>O emission factors from agricultural river  
672 networks based on long-term study at high temporal resolution. *Environ. Sci.*  
673 *Technol.* 53, 10781–10791. <https://doi.org/10.1021/acs.est.9b03896>

674 Tan, L.S., Ge, Z.M., Zhou, X.H., Li, S.H., Li, X.Z., Tang, J.W., 2020. Conversion of  
675 coastal wetlands, riparian wetlands, and peatlands increases greenhouse gas  
676 emissions: A global meta-analysis. *Glob. Change Biol.* 26, 1638–1653.  
677 <http://dx.doi.org/10.1111/gcb.14933>

678 Tian, L.L., Akiyama, H., Zhu, B., Shen, X., 2018. Indirect N<sub>2</sub>O emissions with seasonal  
679 variations from an agricultural drainage ditch mainly receiving interflow water.  
680 *Environ. Pollut.* 242, 480–491. <https://doi.org/10.1016/j.envpol.2018.07.018>

681 Tong, C., Morris, J.T., Huang, J.F., Xu, H., Wan, S.A., 2018. Changes in pore-water  
682 chemistry and methane emission following the invasion of *Spartina alterniflora*  
683 into an oligohaline marsh. *Limnol. Oceanogr.* 63(1), 384–396.  
684 <https://doi.org/10.1002/lno.10637>

685 Turner, P.A., Griffis, T.J., Lee, X., Baker, J.M., Venterea, R.T., Wood, J.D., 2015.  
686 Indirect nitrous oxide emissions from streams within the US Corn Belt scale with  
687 stream order. *PNAS* 112, 9839–9843. <https://doi.org/10.1073/pnas.1503598112>

688 Verhoeven, J.T.A., Setter, T.L., 2010. Agricultural use of wetlands: Opportunities and  
689 limitations. *Ann. Bot.* 105, 155–163. <https://doi.org/10.1093/aob/mcp172>

690 Wang, W.Q., Sardans, J., Wang, C., Zeng, C.S., Tong, C., Asensio, D., Peñuelas, J.,  
691 2017. Relationships between the potential production of the greenhouse gases CO<sub>2</sub>,  
692 CH<sub>4</sub> and N<sub>2</sub>O and soil concentrations of C, N and P across 26 paddy fields in  
693 southeastern China. *Atmos. Environ.* 164, 458–467.  
694 <http://dx.doi.org/10.1016/j.atmosenv.2017.06.023>

695 Wassmann, R., Neue, H.U., Bueno, C., Lantin, R.S., Alberto, M.C.R., Buendia, L.V.,

696 Bronson, K., Papen, H., Rennenberg, H., 1998. [Methane production capacities of](#)  
697 [different rice soils derived from inherent and exogenous substrates](#). *Plant Soil* 203,  
698 [227–237](#).

699 Webb, J.R., Clough, T.J., Quayle, W.C., 2021. A review of indirect N<sub>2</sub>O emission  
700 factors from artificial agricultural waters. *Environ. Res. Lett.* 16, 043005.  
701 <https://doi.org/10.1088/1748-9326/abed00>

702 World Meteorological Organization (WMO), 2021. WMO Greenhouse Gas Bulletin  
703 (GHG Bulletin) - No.17: The State of Greenhouse Gases in the Atmosphere Based  
704 on Global Observations through 2020.  
705 [https://library.wmo.int/doc\\_num.php?explnum\\_id=10904](https://library.wmo.int/doc_num.php?explnum_id=10904)

706 Wu, H.T., Batzer, D.P., Yan, X.M., Lu, X.G., Wu, D.H., 2013. Contributions of ant  
707 mounds to soil carbon and nitrogen pools in a marsh wetland of Northeastern China.  
708 *Appl. Soil Ecol.* 70, 9–15. <https://doi.org/10.1016/j.apsoil.2013.04.004>

709 Wu, Y.Z., Li, Y., Wang, H.H., Wang, Z.J., Fu, X.Q., Shen, J.L., Wang, Y., Liu, X.L.,  
710 Meng, L., Wu, J.S., 2021. Response of N<sub>2</sub>O emissions to biochar amendment on a  
711 tea field soil in subtropical central China: A three-year field experiment. *Agr.*  
712 *Ecosyst. Environ.* 318, 107473. <https://doi.org/10.1016/j.agee.2021.107473>

713 Xie, B., Yu, K.J., 2007. Shrimp farming in China: Operating characteristics,  
714 environmental impact and perspectives. *Ocean Coast. Manage.* 50 (7), 538–550.  
715 <https://doi.org/10.1016/j.ocecoaman.2007.02.006>.

716 Yang, H., Andersen, T., Dörsch, P., Tominaga, K., Thrane, J.E., Hessen, D.O. 2015,  
717 Greenhouse gas metabolism in Nordic boreal lakes. *Biogeochemistry* 126, 211-225.  
718 <https://doi.org/10.1007/s10533-015-0154-8>

719 Yang, P., Lai, D.Y.F., Huang, J.F., Zhang, L.H., Tong, C., 2018. Temporal variations and  
720 temperature sensitivity of ecosystem respiration in three brackish marsh  
721 communities in the Min River Estuary, southeast China. *Geoderma* 327, 138–150.  
722 <https://doi.org/10.1016/j.geoderma.2018.05.005>

723 Yang, P., Lai, D.Y.F., Yang, H., Lin, Y.X., Tong, C., Hong, Y., Tian, Y.L., Tang, C.,  
724 Tang, K.W., 2022a. Large increase in CH<sub>4</sub> emission following conversion of coastal  
725 marsh to aquaculture ponds caused by changing gas transport pathways. *Water Res.*  
726 222, 118882. <https://doi.org/10.1016/j.watres.2022.118882>

- 727 Yang, P., Zhang, Y.F., Yang, H., Guo, Q.Q., Lai, D.Y.F., Zhao, G.H., Li, L., Tong, C.,  
728 2020. Ebullition was a major pathway of methane emissions from the aquaculture  
729 ponds in southeast China. *Water Res.* 184, 116176.  
730 <https://doi.org/10.1016/j.watres.2020.116176>
- 731 Yang, P., Lai, D.Y.F., Jin, B.S., Bastviken, D., Tan, L.S., Tong, C., 2017. Dynamics of  
732 dissolved nutrients in the aquaculture shrimp ponds of the Min River estuary, China:  
733 Concentrations, fluxes and environmental loads. *Sci. Total Environ.* 603-604, 256–  
734 267. <http://dx.doi.org/10.1016/j.scitotenv.2017.06.074>.
- 735 Yang, P., Tang, K.W., Yang, H., Tong, C., Yang, N., Lai, D.Y.F., Hong, Y., Ruan, M.J.,  
736 Tan, Y.Y., Zhao, G.H., Li, L., Tang, C., 2022b. Insights into the farming-season  
737 carbon budget of coastal earthen aquaculture ponds in southeastern China. *Agr.*  
738 *Ecosyst. Environ.* 335, 107995. <https://doi.org/10.1016/j.agee.2022.107995>
- 739 Yang, P., Tang, K.W., Tong, C., Lai, D.Y.F., Wu, L.Z., Yang, H., Zhang, L.H., Tang, C.,  
740 Hong, Y., Zhao, G.H., 2022c. Changes in sediment methanogenic archaea  
741 community structure and methane production potential following conversion of  
742 coastal marsh to aquaculture ponds. *Environm. Pollut.* 305, 119276.  
743 <https://doi.org/10.1016/j.envpol.2022.119276>
- 744 Yang, P., Zhao, G.H., Tong, C., Tang, K.W., Lai, D.Y.F., Li, L., Tang, C., 2021.  
745 Assessing nutrient budgets and environmental impacts of coastal land-based  
746 aquaculture system in southeastern China. *Agr. Ecosyst. Environ.* 322, 107662.  
747 <https://doi.org/10.1016/j.agee.2021.107662>
- 748 Yang, P., Wang, M.H., Lai, D.Y.F., Chun, K.P., Huang, J.F., Wan, S.A., Bastviken, D.,  
749 Tong, C., 2019. Methane dynamics in an estuarine brackish *Cyperus malaccensis*  
750 marsh: Production and porewater concentration in soils, and net emissions to the  
751 atmosphere over five years. *Geoderma* 337, 132–142.  
752 <https://doi.org/10.1016/j.geoderma.2018.09.019>
- 753 Yeung, L.Y., Haslun, J.A., Ostrom, N.E., Sun, T., Young, E.D., van Kessel, M.A.H.J.,  
754 Lückner, S., Mike Jetten, S.M., 2019. In situ quantification of biological N<sub>2</sub>  
755 production using naturally occurring <sup>15</sup>N<sup>15</sup>N. *Environ. Sci. Technol.* 53(9), 5168–  
756 5175. <https://doi.org/10.1021/acs.est.9b00812>
- 757 Yuan, J.J., Liu, D.Y., Xiang, J., He, T.H., Kang, H., Ding, W.X., 2021. Methane and

758 nitrous oxide have separated production zones and distinct emission pathways in  
759 freshwater aquaculture ponds. *Water Res.* 190, 116739.  
760 <https://doi.org/10.1016/j.watres.2020.116739>

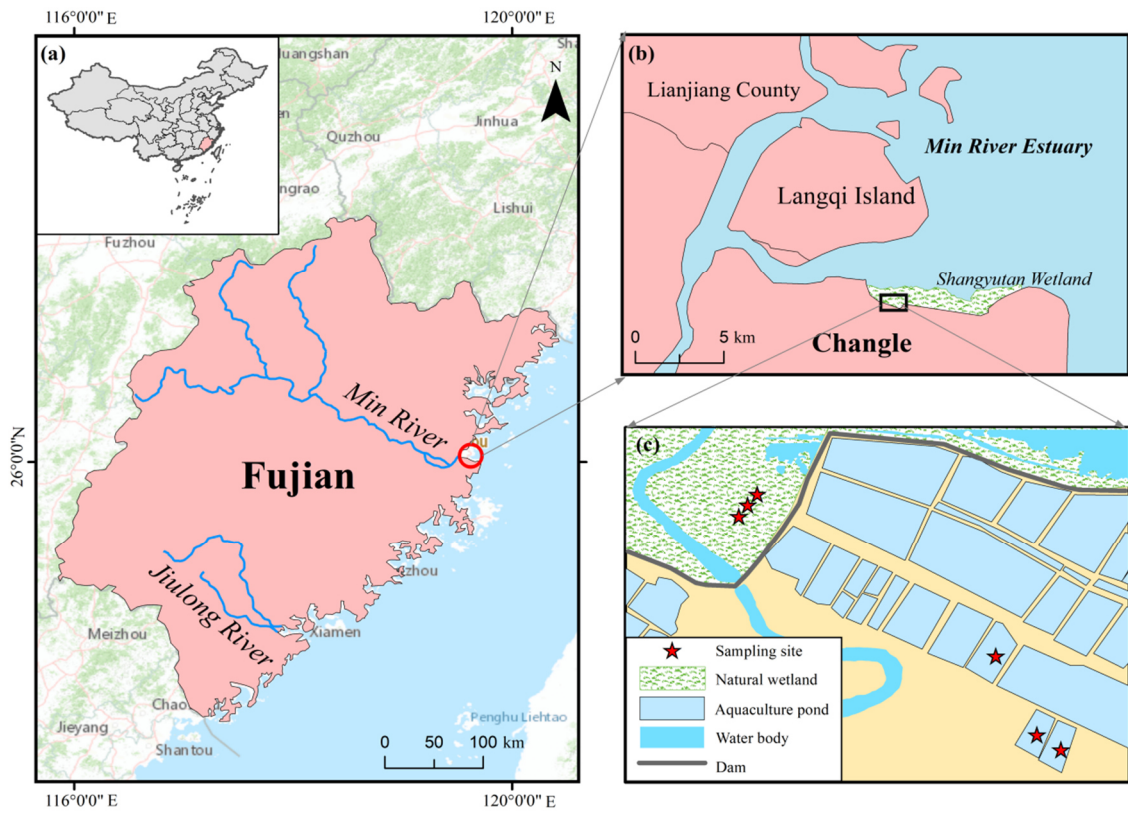
761 Yuan, J.J., Xiang, J., Liu, D.Y., Kang, H., He, T.H., Kim, S., Lin, Y.X., Freeman, C.,  
762 Ding, W.X., 2019. Rapid growth in greenhouse gas emissions from the adoption of  
763 industrial-scale aquaculture. *Nat. Clim. Change* 9(4), 318–322.  
764 <https://doi.org/10.1038/s41558-019-0425-9>

765 Zhou, M.H., Wang, X.G., Ke, Y., Zhu, B., 2019. Effects of afforestation on soil nitrous  
766 oxide emissions in a subtropical montane agricultural landscape: A 3-year field  
767 experiment. *Agr. Forest Meteorol.* 266–267, 221–230.  
768 <https://doi.org/10.1016/j.agrformet.2019.01.003>

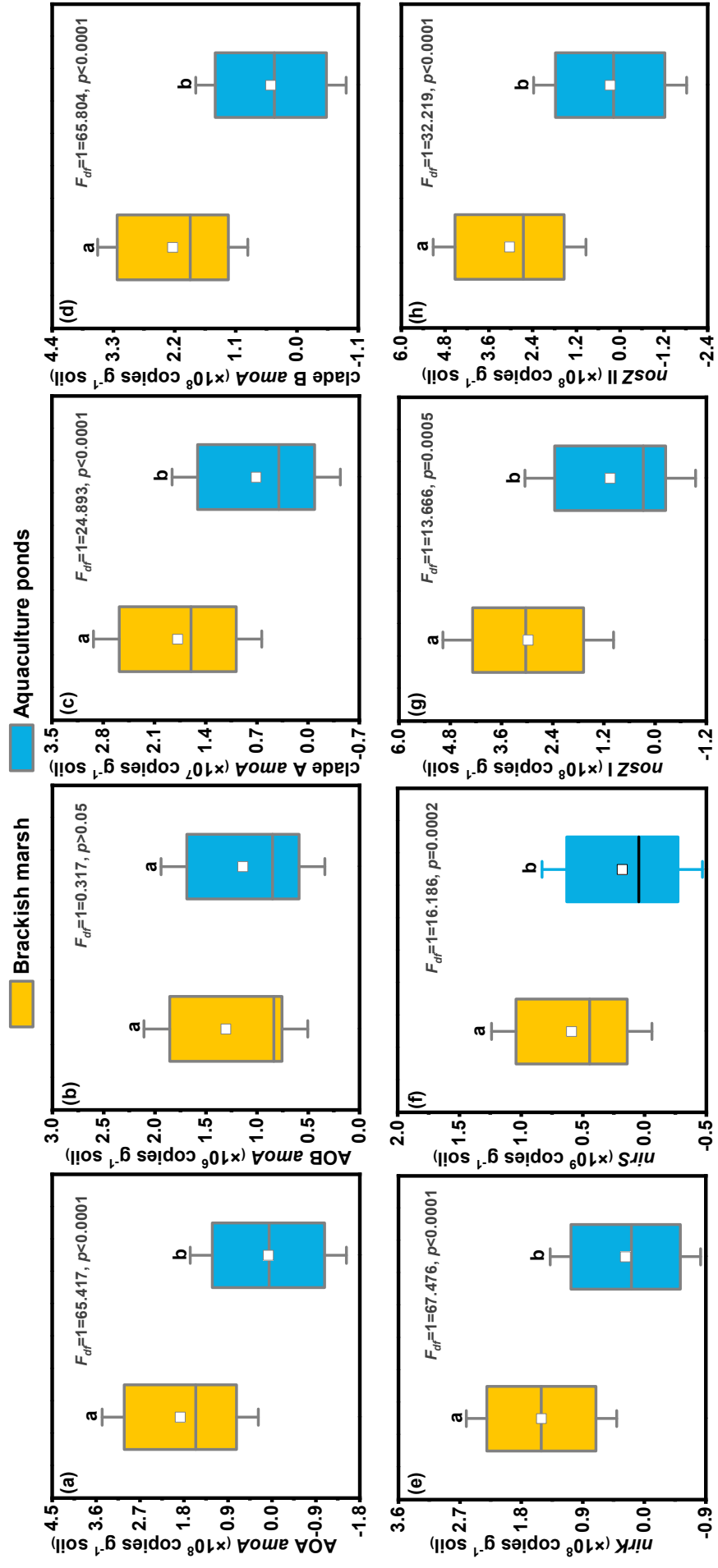
1 **Table 1**

2 Physico-chemical properties of the sediments and porewater in the brackish marsh and aquaculture ponds. Different lowercase letters within the  
 3 same column indicate significant differences between the two habitats ( $p < 0.05$ ). See main text for explanation of the abbreviations.

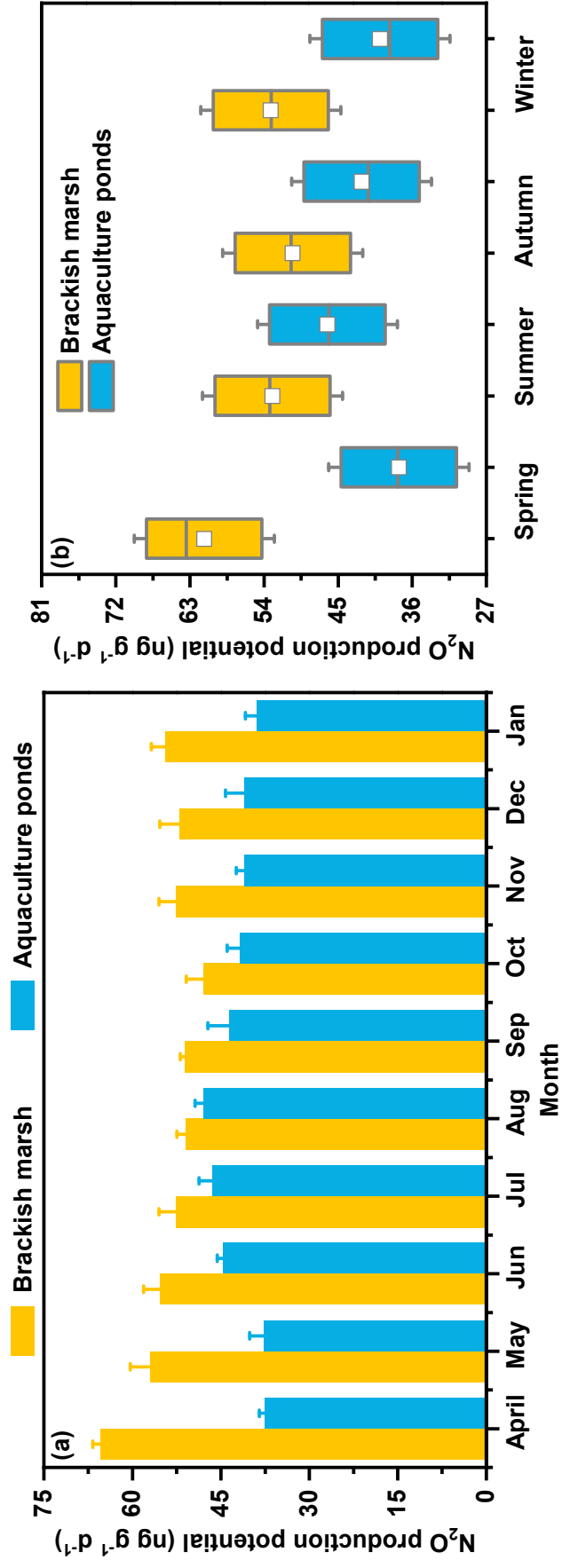
Habitat types	Sediment physicochemical parameters				Porewater physicochemical parameters			
	$T_s$ (°C)	pH	Salinity (‰)	TN (g kg <sup>-1</sup> )	C:N ratio	NO <sub>3</sub> <sup>-</sup> -N (mg L <sup>-1</sup> )	NH <sub>4</sub> <sup>+</sup> -N (mg L <sup>-1</sup> )	SO <sub>4</sub> <sup>2-</sup> (mg L <sup>-1</sup> )
Brackish marsh	24.70±0.85 <sup>a</sup>	6.72±0.12 <sup>a</sup>	6.69±0.63 <sup>a</sup>	1.34±0.09 <sup>a</sup>	13.07±0.87 <sup>a</sup>	0.51±0.05 <sup>a</sup>	0.48±0.05 <sup>a</sup>	935.24±98.61 <sup>a</sup>
Aquaculture ponds	20.42±0.62 <sup>b</sup>	6.75±0.04 <sup>a</sup>	2.51±0.16 <sup>b</sup>	0.70±0.07 <sup>b</sup>	28.08±3.22 <sup>b</sup>	0.22±0.03 <sup>b</sup>	0.33±0.04 <sup>b</sup>	780.38±78.51 <sup>a</sup>



1  
 2 **Figure 1.** Map of the Shanyutan Wetland within the Min River Estuary showing the  
 3 sampling sites in the brackish marsh and aquaculture ponds reclaimed from the marsh.

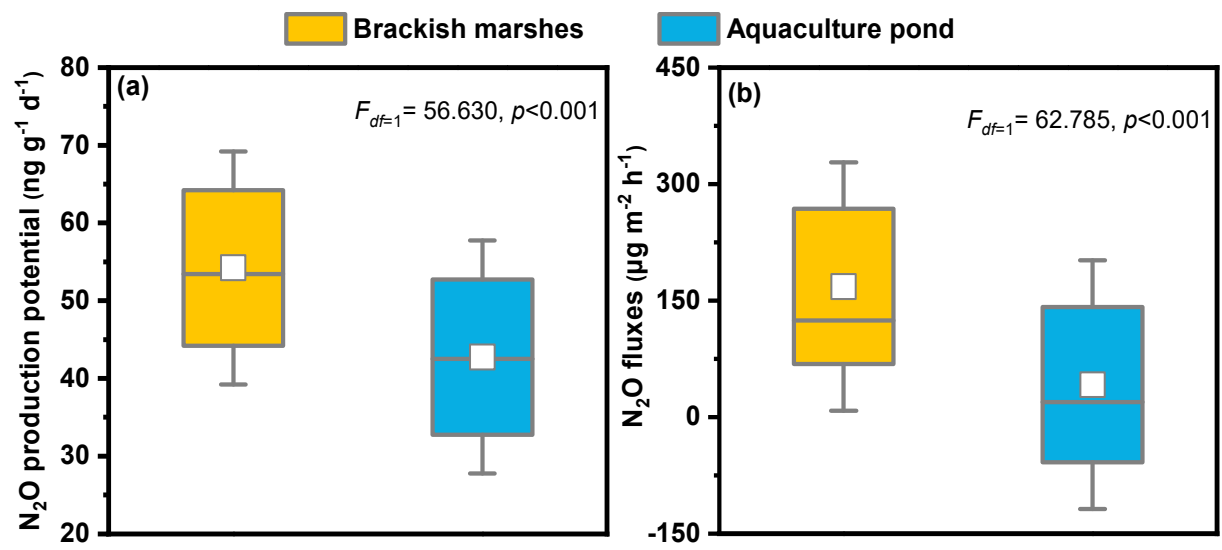


4  
5 **Figure 2.** Boxplots of gene abundance (AOA amoA, AOB amoA, comammox Nitrospira clades A and B amoA, nirK, nirS, nosZ I and nosZ II) in  
6 surface sediment in the brackish marsh and the aquaculture ponds. Different letters above the boxes indicate significant differences ( $p < 0.05$ )  
7 between the two habitats.



8

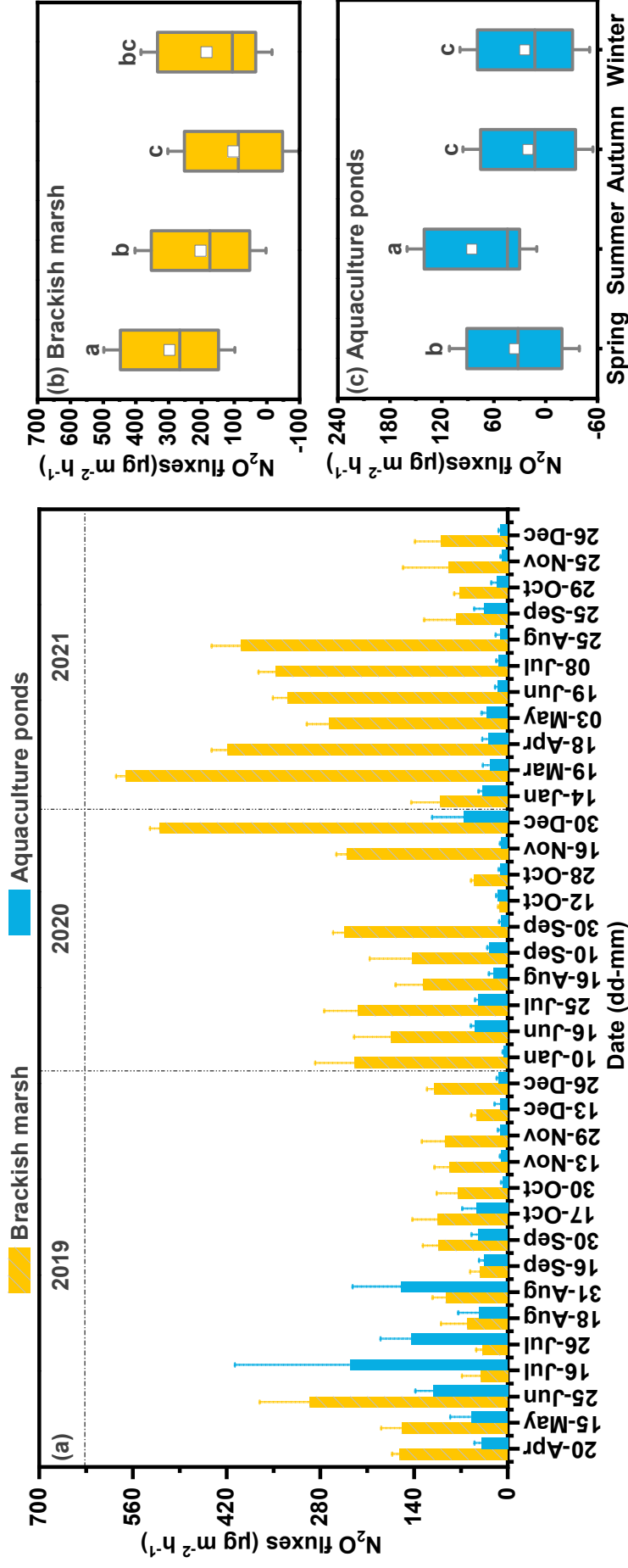
9 **Figure 3.** Sediment N<sub>2</sub>O production potentials plotted as (a) monthly values (mean ± SE) between 2019 and 2021 and (b) boxplots of  
 10 seasonal values in the brackish marsh and the aquaculture ponds.



11

12 **Figure 4.** Boxplots of (a) sediment N<sub>2</sub>O production potentials and (b) N<sub>2</sub>O emission fluxes in

13 the brackish marsh and aquaculture ponds.

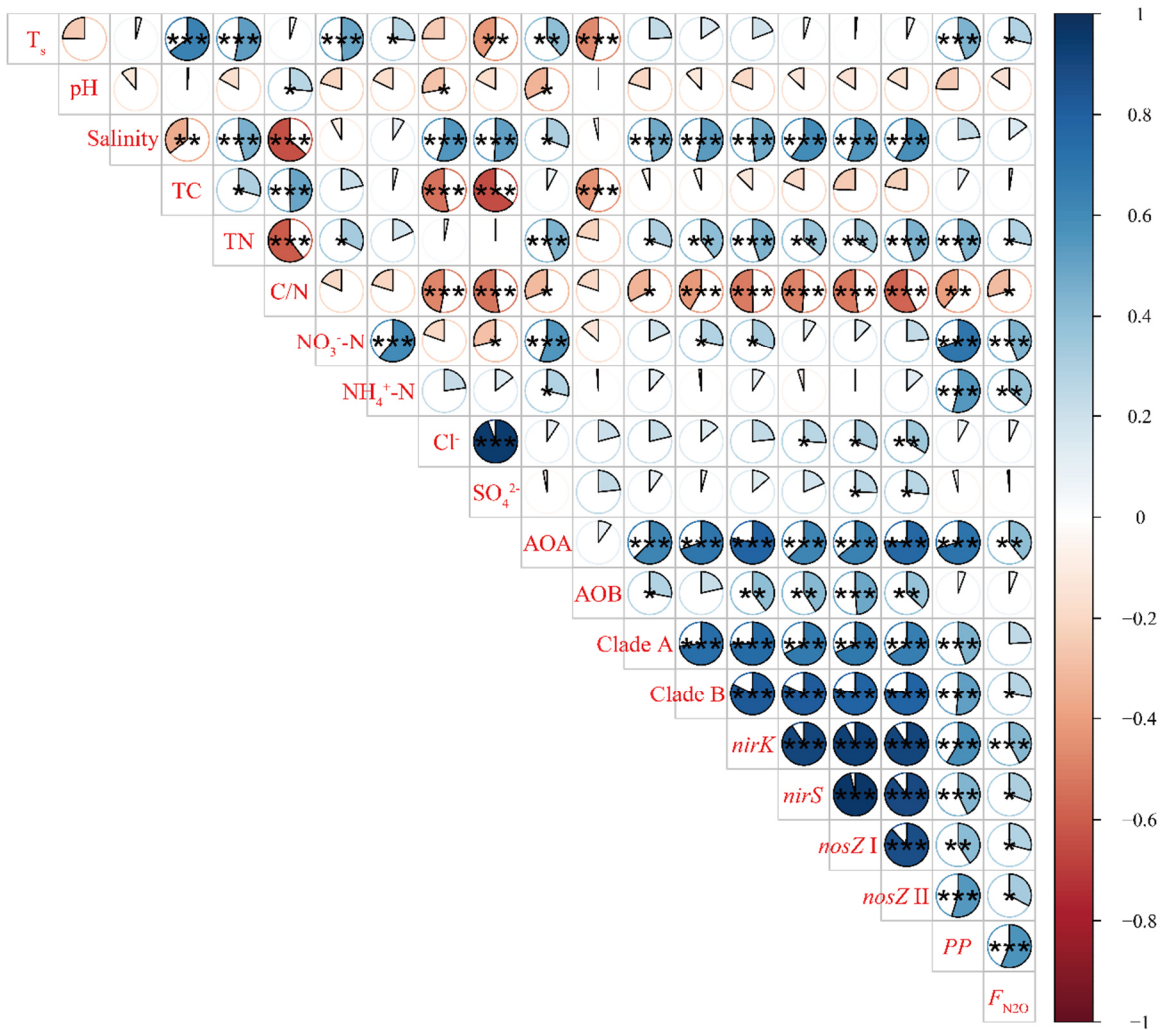


14

15 **Figure 5.**  $N_2O$  emission fluxes (a) measured on different dates (mean  $\pm$  SE) in the brackish marsh and aquaculture ponds over a three-year period;

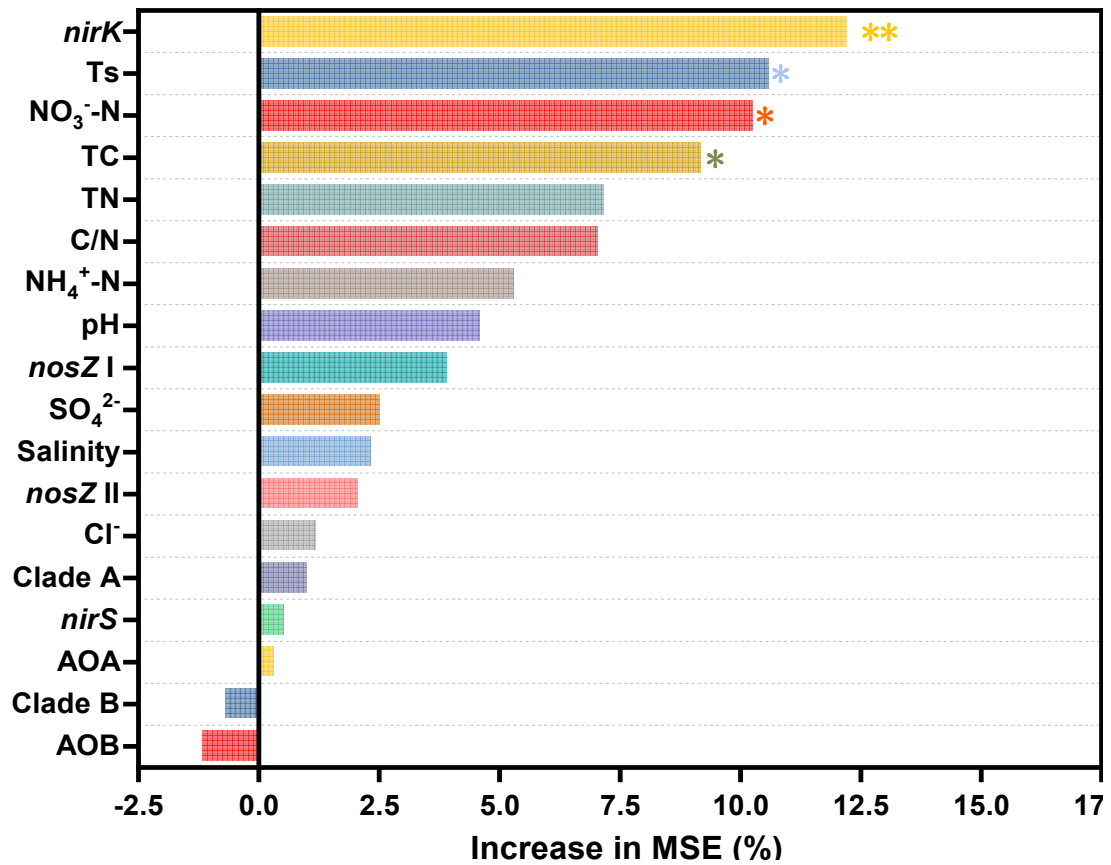
16 (b) plotted as boxplots of seasonal values for the brackish marsh; and (c) plotted as boxplots of seasonal values for the aquaculture ponds. Different

17 letters above the boxes indicate significant differences between seasons ( $p < 0.05$ ).



18

19 **Figure 6.** Correlations among environmental variables, abundance of major N-cycling  
 20 functional genes, sediment N<sub>2</sub>O production potential (*PP*) and N<sub>2</sub>O emission flux (*F<sub>N2O</sub>*)  
 21 ( $n = 60$ ). Colors of the circle segments indicate the direction of correlation (blue =  
 22 positive; red = negative). Size of the colored segment is proportional to the  $r$  value.  
 23 Asterisks indicate levels of significance (\* $p < 0.05$ ; \*\* $p < 0.01$ ; \*\*\* $p < 0.001$ ). See main  
 24 text for explanation of the abbreviations.



25

26 **Figure 7.** Random forest predictor importance, as measured by percent increase in mean  
 27 square error (MSE) of N<sub>2</sub>O emission. Asterisks indicate levels of significance (\**p* < 0.05;  
 28 \*\**p* < 0.01). See main text for explanation of the abbreviations.

1 **Supporting Information**

2 **Conversion of coastal wetland to aquaculture ponds decreased N<sub>2</sub>O**  
3 **emission: Evidence from a multi-year field study**

4 Ping Yang<sup>a,b\*</sup>, Kam W. Tang<sup>c</sup>, Chuan Tong<sup>a,b\*</sup>, Derrick Y.F. Lai<sup>d</sup>, Linhai  
5 Zhang<sup>a,b</sup>, Xiao Lin<sup>a,b</sup>, Hong Yang<sup>e,f</sup>, Lishan Tan<sup>g</sup>, Yifei Zhang<sup>a</sup>, Yan Hong<sup>a</sup>,  
6 Chen Tang<sup>a</sup>, Yongxin Lin<sup>a,b\*</sup>

7 <sup>a</sup>*School of Geographical Sciences, Fujian Normal University, Fuzhou 350007, P.R. China*

8 <sup>b</sup>*Key Laboratory of Humid Subtropical Eco-geographical Process of Ministry of Education,*  
9 *Fujian Normal University, Fuzhou 350007, P.R. China*

10 <sup>c</sup>*Department of Biosciences, Swansea University, Swansea SA2 8PP, U. K.*

11 <sup>d</sup>*Department of Geography and Resource Management, The Chinese University of Hong*  
12 *Kong, Hong Kong, China*

13 <sup>e</sup>*College of Environmental Science and Engineering, Fujian Normal University, Fuzhou*  
14 *350007, P.R. China*

15 <sup>f</sup>*Department of Geography and Environmental Science, University of Reading, Reading,*  
16 *RG6 6AB, UK*

17 <sup>g</sup>*State Key Laboratory of Estuarine and Coastal Research, East China Normal University,*  
18 *Shanghai, China*

19

20 **\*Correspondence to:**

21 Ping Yang ([yangping528@sina.cn](mailto:yangping528@sina.cn)); Chuan Tong ([tongch@fjnu.edu.cn](mailto:tongch@fjnu.edu.cn)); Yongxin Lin  
22 ([yxlin@fjnu.edu.cn](mailto:yxlin@fjnu.edu.cn))

23 **Telephone:** 086-0591-87445659 **Fax:** 086-0591-83465397

24 **Supporting Information Summary**

25 **No. of pages: 8**    **No. of figures: 3**    **No. of tables: 2**

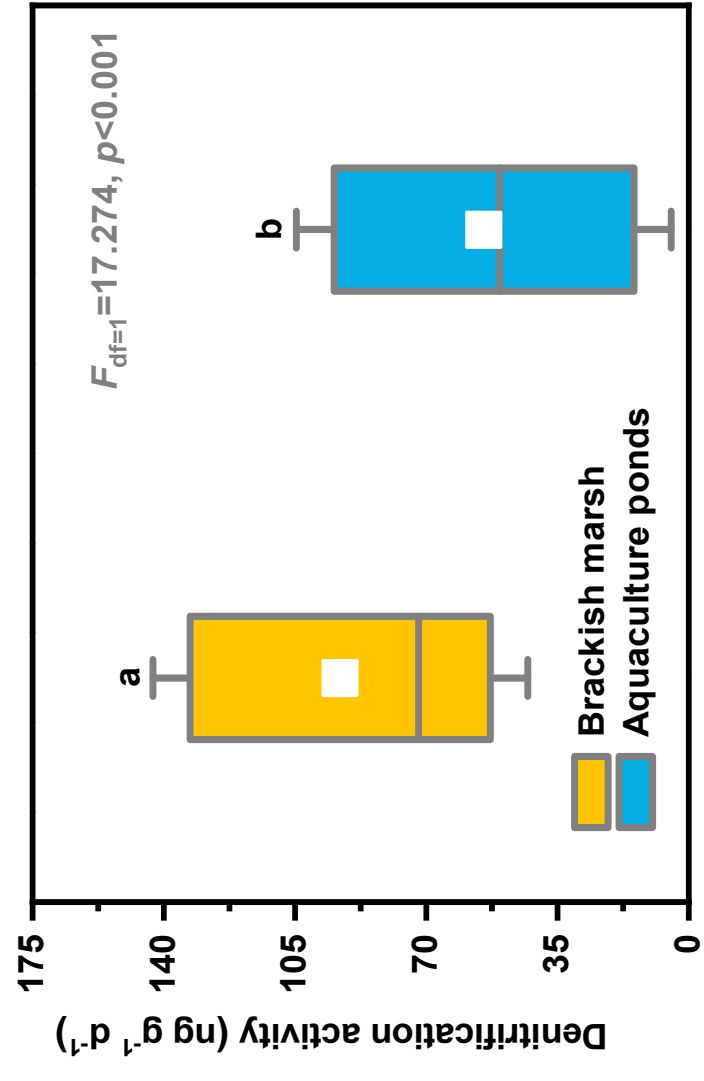
26 **Page S3:** Figure S1. Boxplots of sediment potential denitrification activity (SPDA) in  
27 the brackish marsh and aquaculture ponds.

28 **Page S4:** Figure S2. Redundancy analysis (RDA) biplots of sediment N<sub>2</sub>O production  
29 potentials (*PP*) and N<sub>2</sub>O emission fluxes ( $F_{N_2O}$ ) in (a) the marsh; and (b) the aquaculture  
30 ponds, showing the loadings of ancillary environmental variables (black arrows) and the  
31 scores of observations in all sampling campaigns. The pie charts show the percentages  
32 of N<sub>2</sub>O production potentials (or N<sub>2</sub>O emission fluxes) variances explained by the  
33 different variables. See main text for explanation of the abbreviations.

34 **Page S5:** Figure S3. Relationships between sediment N<sub>2</sub>O production potentials and  
35 abundances of N-cycling functional genes in the marsh and aquaculture ponds.  
36 Significant linear regressions are included where applicable.

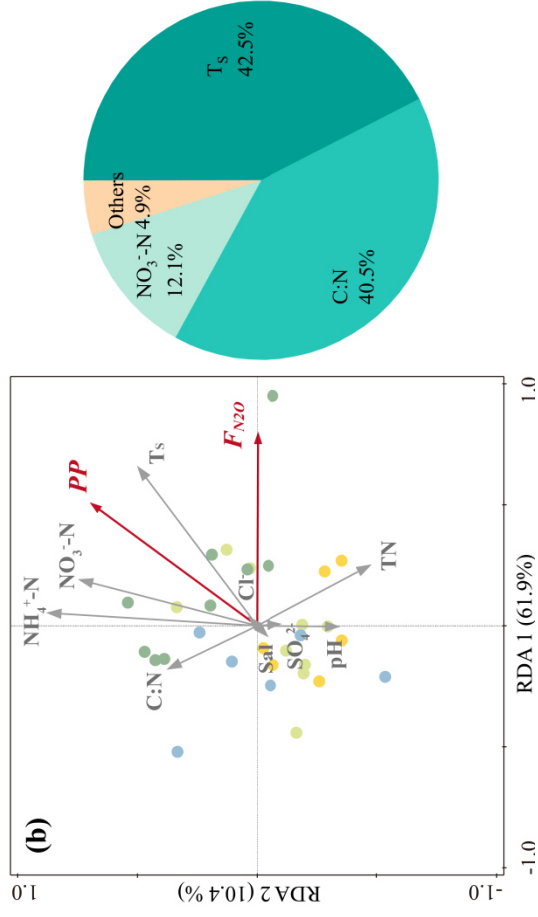
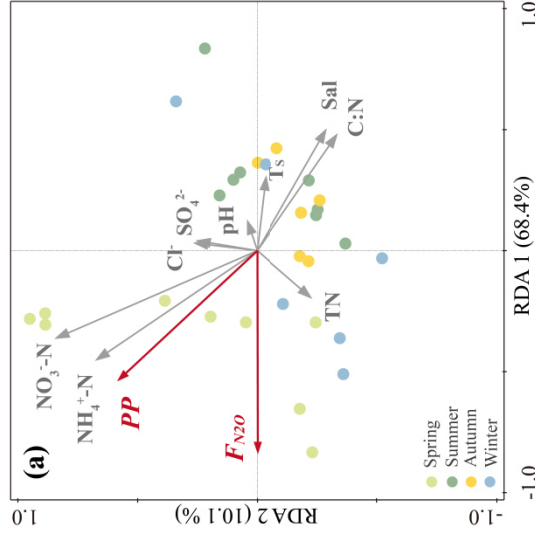
37 **Page S6:** Table S1 PCR primers and thermal cycling conditions used for gene  
38 quantification.

39 **Page S7:** Table S2 Pearson correlation coefficients between sediment N<sub>2</sub>O production  
40 potential, N<sub>2</sub>O emission flux and different environmental variables in the marsh and  
41 aquaculture ponds in this study. Significant correlations are indicated by the symbols \*  
42 ( $p < 0.05$ ) and \*\* ( $p < 0.01$ ).



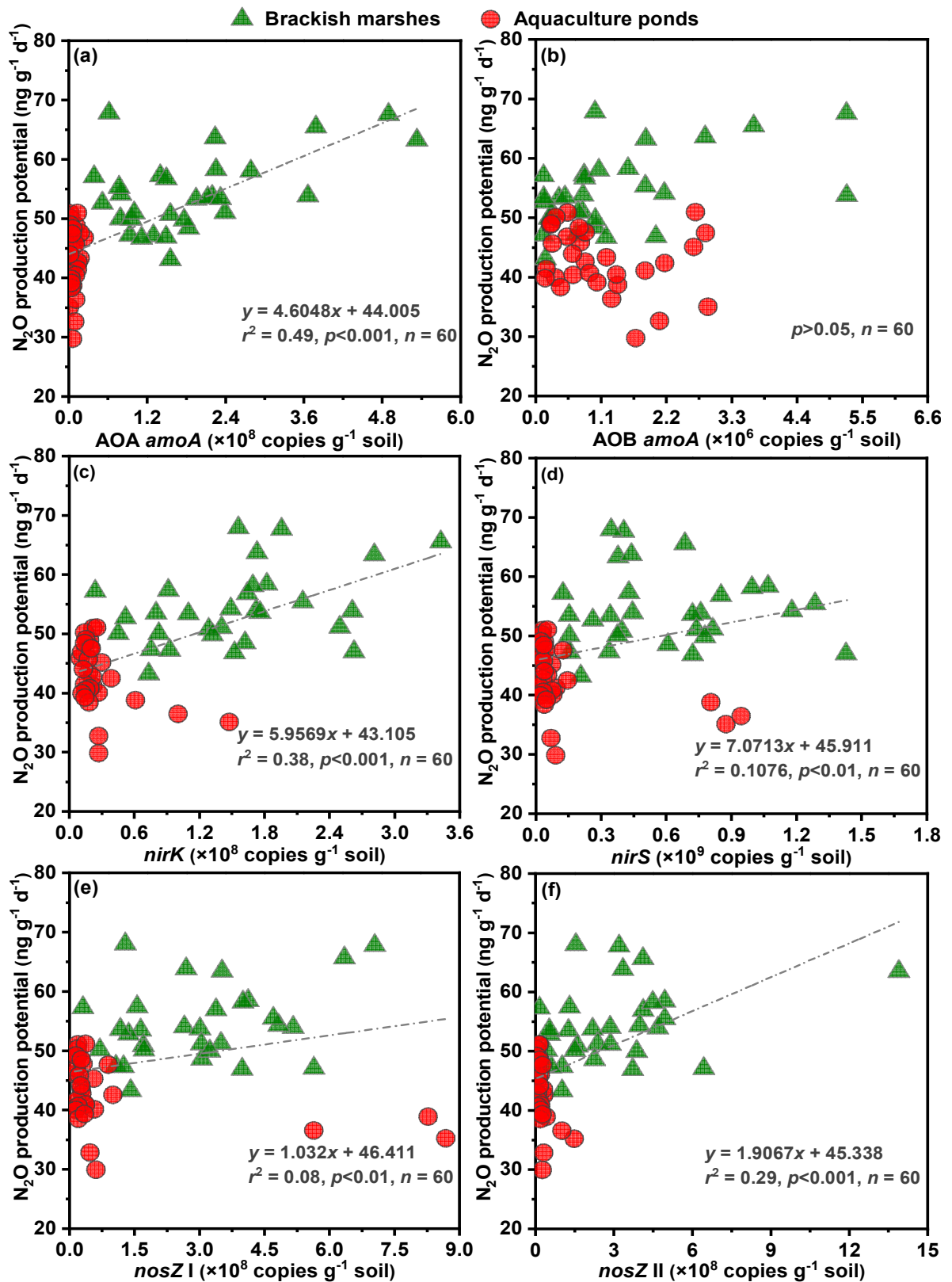
43

44 **Figure S1.** Boxplots of sediment potential denitrification activity (SPDA) in the brackish  
 45 marsh and aquaculture ponds.



46

47 **Figure S2.** Redundancy analysis (RDA) biplots of sediment N<sub>2</sub>O production potentials (*PP*) and N<sub>2</sub>O emission fluxes (*F<sub>N2O</sub>*) in (a) the marsh; and  
 48 (b) the aquaculture ponds, showing the loadings of ancillary environmental variables (black arrows) and the scores of observations in all sampling  
 49 campaigns. The pie charts show the percentages of N<sub>2</sub>O production potentials (or N<sub>2</sub>O emission fluxes) variances explained by the different  
 50 variables. See main text for explanation of the abbreviations.



51

52 **Figure S3.** Relationships between sediment  $N_2O$  production potentials and abundances

53 of N-cycling functional genes in the marsh and aquaculture ponds. Significant linear

54 regressions are included where applicable.

55 **Table S1**

56 PCR primers and thermal cycling conditions used for gene quantification.

Gene	Primer	Sequence	Thermal conditions	Amplification efficiency (%)	Reference
<b>AOA</b>	Arch- <i>amoA</i> F	STAATGGTCTGGCTTAGACG	95°C, 3min; 35× (95°C for 10 s, 55°C for 30 s, 72°C for 45 s+ plate read) ; Melt curve: 65.0°C to 95.0°C, increment 0.5°C, 0:05+ plate read	101.2–102.1	Francis et al., 2005
<i>amoA</i>	Arch- <i>amoA</i> R	GCGGCCCATCCATCTGTAT GT			
<b>AOB</b>	amoA-1F	GGGGTTTCTACTGGTGGT	95°C, 3min; 35× (95°C for 10 s, 55°C for 30 s, 72°C for 45 s+ plate read) ; Melt curve: 65.0°C to 95.0°C, increment 0.5°C, 0:05+ plate read	96.3–97.0	Rothhauwe et al., 1997
<i>amoA</i>	amoA-2R	CCC CTC KGS AAA GCCTTCTTC			
<b>Clade A</b>	CA377f	GTGGTGGTGGTCBAAAYTA	95°C, 3min; 35 × (95°C for 30 s, 55°C for 25 s, 72°C for 20 s); Melt curve: 65.0°C to 95.0°C increment 0.5°C, 0:05	89.6–91.1	Jiang et al., 2020
<i>amoA</i>	C576r	GAAGCCCATRTARTCNGCC			
<b>Clade B</b>	CB377f	GTACTGGTGGGCBAAYTT	95°C, 3min; 35 × (95°C for 30 s, 55°C for 25 s, 72°C for 20 s); Melt curve: 65.0°C to 95.0°C increment 0.5°C, 0:05	78.8–81.4	Jiang et al., 2020
<i>amoA</i>	C576r	GAAGCCCATRTARTCNGCC			
<b>nirS</b>	nirSCd3aF	GTSAACGTSAAAGGARACSGG	95°C, 3 min; 35× (95°C for 10 s, 56 °C for 30 s, 72°C for 20 s+ plate read) ; Melt curve: 65.0°C to 95.0°C, increment 0.5°C, 0:05+ plate read	97.1–97.8	Throback et al., 2004
	nirSR3cd	GASTTCGGRTGSGTCTTGA			
	nirKF1aCu	ATCATGGTSC TGCCGCG	95°C, 3 min; 35× (95°C for 10 s, 56 °C for 30 s, 72°C for 20 s+ plate read) ; Melt curve: 65.0°C to 95.0°C, increment 0.5°C, 0:05+ plate read	90.4–91.8	Throback et al., 2004
<b>nirK</b>	nirKR3Cu	GCCTCGATCAGRTTGTGGTT			

<b><i>nosZ I</i></b>	nosZ1840F	CGCRACGGCAASAAGGTSMSSGT	95°C, 3 min; 35× (95°C for 10 s, 58 °C for 25 s, 93.0–93.8 °C for 20 s+ plate read) ; Melt curve: 65.0°C to 95.0°C, increment 0.5°C, 0:05+ plate read	Henry et al., 2006
	nosZ2090R	CAKRTGCAKSGCRTGGCAGAA		
<b><i>nosZ II</i></b>	nosZ-II-F	CTIGGICCIYTKCAYAC	95°C, 3 min; 35× (95°C for 10 s, 54 °C for 30 s, 90.7–91.4 °C for 40 s+ plate read) ; Melt curve: 65.0°C to 95.0°C, increment 0.5°C, 0:05+ plate read	Jones et al., 2013
	nosZ-II-R	GCIGARCARAAITCBGTRC		

58 **Table S2**

59 Pearson correlation coefficients between sediment N<sub>2</sub>O production potential, N<sub>2</sub>O emission flux and different environmental variables in the  
 60 marsh and aquaculture ponds in this study. Significant correlations are indicated by the symbols \* ( $p < 0.05$ ) and \*\* ( $p < 0.01$ ).

Environmental variables	Brackish marsh		Aquaculture ponds	
	N <sub>2</sub> O production potential	N <sub>2</sub> O emission flux	N <sub>2</sub> O production potential	N <sub>2</sub> O emission flux
<b>Sediment parameters</b>				
Sediment temperature ( <i>T</i> s)	-0.181	-0.250	<b>0.669**</b>	<b>0.513**</b>
pH	-0.040	-0.099	-0.236	-0.001
Salinity	<b>-0.430*</b>	<b>-0.411*</b>	-0.048	-0.032
Total nitrogen (TN)	-0.026	0.161	-0.200	0.198
C:N ratio	<b>-0.445*</b>	<b>-0.394*</b>	0.165	-0.141
<b>Porewater parameters</b>				
NO <sub>3</sub> <sup>-</sup> -N	<b>0.674**</b>	0.298	<b>0.604**</b>	0.147
NH <sub>4</sub> <sup>+</sup> -N	<b>0.626**</b>	<b>0.372*</b>	<b>0.626**</b>	0.039
Cl <sup>-</sup>	0.133	-0.026	0.039	0.026
SO <sub>4</sub> <sup>2-</sup>	0.122	-0.034	-0.063	0.006

61

## 62 Reference

- 63 Francis, C.A., Roberts, K.J., Beman, J.M., Santoro, A.E., Oakley, B.B., 2005. Ubiquity and  
64 diversity of ammonia oxidizing archaea in water columns and sediments of the ocean. P.  
65 Natl. Acad. Sci. USA 102, 14683–14688. <https://doi.org/10.1073/pnas.0506625102>
- 66 Henry, S., Bru, D., Stres, B., Hallet, S., Philippot, L., 2006. Quantitative detection of the *nosZ*  
67 gene, encoding nitrous oxide reductase, and comparison of the abundances of 16S rRNA,  
68 *narG*, *nirK*, and *nosZ* genes in soils. Appl. Environ. Microb. 72, 5181–5189.  
69 <https://doi.org/10.1128/AEM.00231-06>
- 70 Jiang R, Wang JG, Zhu T, Zou B, Wang DQ, Rhee SK, An D, Ji ZY, Quan ZX (2020) Use of  
71 newly designed primers for quantification of complete ammonia-oxidizing (comammox)  
72 bacterial clades and strict nitrite oxidizers in the genus *Nitrospira*. Appl. Environ. Microb.  
73 86:e01775–01720. <https://doi.org/10.1128/AEM.01775-20>
- 74 Jones, C.M., Graf, D.R.H., Bru, D., Philippot, L., Hallin, S., 2013. The unaccounted yet  
75 abundant nitrous oxide-reducing microbial community: a potential nitrous oxide sink.  
76 ISME J. 7, 417–426. <https://doi.org/10.1038/ismej.2012.125>
- 77 Rotthauwe, J.H., Witzel, K.P., Liesack, W., 1997. The ammonia monooxygenase structural  
78 gene *amoA* as a functional marker: molecular fine-scale analysis of natural ammonia-  
79 oxidizing populations. Appl. Environ. Microb. 63, 4704–4712.  
80 <https://doi.org/10.1128/aem.63.12.4704-4712.1997>
- 81 Throbäck, I.N., Enwall, K., Jarvis, Å., Hallin, S., 2004. Reassessing PCR primers targeting  
82 *nirS*, *nirK* and *nosZ* genes for community surveys of denitrifying bacteria with DGGE.  
83 FEMS Microbiol. Ecol. 49, 401–417. <https://doi.org/10.1016/j.femsec.2004.04.011>